

Selection of functional predictors and smooth coefficient estimation for scalar-on-function regression models

Hedayat Fathi

Department of Operations and Decision Systems, Université Laval, Québec, Canada
hedayat.fathi.1@ulaval.ca

Marzia A. Cremona

Chair in Statistical Learning and Department of Operations and Decision Systems, Université Laval,
 Québec, Canada
marzia.cremona@fsa.ulaval.ca

Federico Severino

Department of Finance, Insurance and Real Estate, Université Laval, Québec, Canada
federico.severino@fsa.ulaval.ca

Abstract

In the framework of scalar-on-function regression models, in which several functional variables are employed to predict a scalar response, we propose a methodology for selecting relevant functional predictors while simultaneously providing accurate smooth (or more generally regular) estimates of the functional coefficients. We suppose that the functional predictors belong to a real separable Hilbert space, while the functional coefficients belong to a specific subspace of this Hilbert space. Such a subspace can be a Reproducing Kernel Hilbert Space (RKHS) to ensure the desired regularity characteristics, such as smoothness or periodicity, for the coefficient estimates. Our procedure, called SOFIA (Scalar-On-Function Integrated Adaptive Lasso), is based on an adaptive penalized least squares algorithm that leverages functional subgradients to efficiently solve the minimization problem. We demonstrate that the proposed method satisfies an appropriate version of the oracle property adapted to the functional setting, even when the number of predictors exceeds the sample size. SOFIA's effectiveness in variable selection and coefficient estimation is evaluated through extensive simulation studies and a real-data application to predict GDP growth.

Acknowledgments: We thank Ana Maria Kenney, Michael Morin, Hans-Georg Müller, Matthew Reimherr, Bharath Sriperumbudur and Ruodu Wang, as well as participants at the Second Workshop Mathematics for Artificial Intelligence and Machine Learning (Università Bocconi, 2024), at the 2024 Annual Meeting of the Statistical Society of Canada (Memorial University of Newfoundland), at the Canadian Mathematical Society Summer Meeting 2025 (Québec), at the 2025 International Conference on Statistics and Data Science (Vancouver) and at Université Laval (2025) for useful comments. Hedayat Fathi acknowledges the support of the Faculty of Business Administration, Université Laval, and of the Interuniversity Research Center on Enterprise Network, Logistics and Transportation (CIRRELT). Marzia A. Cremona acknowledges the support of the Natural Sciences and Engineering Research Council of Canada (NSERC, grant RGPIN-2020-05657), of the Fonds de recherche du Québec Santé (FRQS, grant 2023-2024-JC-339901), of the Social Sciences and Humanities Research Council (SSHRC, grant 430-2020-00358) and of the Faculty of Business Administration, Université Laval. Federico Severino acknowledges the financial support of the Social Sciences and Humanities Research Council (SSHRC, grant 430-2020-00358). This research was enabled by the computing capability of the Digital Research Alliance of Canada.

Keywords: Variable selection, Scalar-on-function regression, Functional Data Analysis, Reproducing Kernel Hilbert Spaces, Regularization, Oracle property
MSC classification: primary 62R10, 62J05; secondary 46E22.

1 Introduction

High-dimensional regression models are crucial in modern data analysis and have numerous applications in several fields such as genetics, finance, and the social sciences. In the extreme case, some or all of the variables included in the model are functions that vary over a continuum, such as time or space. The use of functional data can result in more accurate data analysis, improved pattern extraction, and enhanced visualization. However, functional data also introduce new challenges in statistical modeling. For example, in functional regression models involving a large number of predictors, selecting the most relevant ones is needed to improve model interpretability and predictive accuracy, as well as to reduce computational complexity (see, e.e, Campos-Sánchez et al., 2016; Chen et al., 2020). Standard references for functional data analysis (FDA) are Ramsay and Silverman (2005) and Kokoszka and Reimherr (2017).

There exist three main types of functional linear regression models: scalar response with functional predictors, functional response with scalar predictors, and functional response with functional predictors. In this study, we focus on the first category, known as *scalar-on-function regression*, and introduce a new approach to simultaneously perform variable selection and smooth coefficient estimation. In particular, we consider the standardized regression model

$$Y_i = \sum_{j=1}^p \langle \beta_j^*, X_{ij} \rangle_{\mathbb{H}} + \varepsilon_i, \quad i = 1, \dots, n, \quad (1)$$

where Y_i is the scalar response, X_{ij} are the p functional predictors belonging to a real separable Hilbert space $(\mathbb{H}, \langle \cdot, \cdot \rangle_{\mathbb{H}})$ (in the simplest case $L^2[0, 1]$), ε_i are independent scalar random errors with mean 0 and variance σ^2 , and n is the sample size. For each j , the function β_j^* quantifies the effect of the j^{th} functional predictor on the scalar response. Applications of scalar-on-function regression are widespread, including finance (where curves are time series), medicine, and the natural sciences (Ullah and Finch, 2013). Although variable selection methods for classic linear regression models are ubiquitous in the statistical literature (see two recent examples in Insolia et al., 2022; Hanke et al., 2024), they have only recently been extended to the functional setting (Aneiros et al., 2022).

In this paper, we focus on situations where several functional predictors are present but only a small number among them are active (i.e., have $\beta_j^* \neq 0$). Even in classical multiple regression models (where no functional variable is involved), when the number of predictors is large, best subset selection may be computationally infeasible and stepwise selection provides only locally optimal solutions to the variable selection problem. Lasso can be effective in practice (Tibshirani, 1996), but does not satisfy the oracle property (Fan and Li, 2001). The adaptive lasso method (Zou, 2006) adds a data-driven weighting scheme to the penalty term of lasso to improve the accuracy of the estimates and ensure the validity of an oracle property. Under appropriate assumptions, the adaptive lasso is an oracle estimator even when the number of predictors increases with the sample size (Huang et al., 2008). Following this literature, in this paper, we propose an adaptive lasso method for scalar-on-function regression that simultaneously performs variable selection and coefficient function estimation, ensuring a desired level of regularity for the coefficients. First, we employ a functional version of (non-adaptive) lasso to filter out some variables and obtain initial

estimates of the coefficients for the selected predictors. Second, similarly to adaptive lasso, we set weights as reciprocals of the absolute values of the obtained estimates. The primary challenge in the scalar-on-function setting is that the design matrix does not consist of scalar entries but contains elements of a Hilbert space. This difference introduces several computational and theoretical challenges. To avoid redundancy in terminology, we refer to our method as *SOFIA-Lasso* (Scalar-On-Function Integrated Adaptive Lasso), or simply *SOFIA*. The term *integrated* reflects the integration of two norms, enabling the simultaneous selection of variables and regularization of functional coefficients. From an asymptotical point of view, SOFIA enjoys an oracle property even in the case where the number of variables and the number of active predictors increase as the sample size increases. Specifically, we allow the number of predictors to grow faster than the sample size (even at an exponential rate). The challenges of such situations in multiple regression models are illustrated in Huang et al. (2008).

In our framework, while predictors belong to a general Hilbert space \mathbb{H} , we assume that coefficient functions β_j^* belong to a specific dense Hilbert subspace \mathbb{K} that incorporates desirable regularity properties such as smoothness or periodicity. This subspace is defined by the eigenfunctions of a positive self-adjoint operator K on \mathbb{H} . When a positive-definite kernel induces the operator K , the resulting space forms a reproducing kernel Hilbert space (RKHS; see definitions in Hsing and Eubank, 2015). Hence, we consider a generalization of the RKHS setting which offers greater flexibility. This framework pursues two primary objectives. First, by choosing an appropriate operator K , we ensure the desired level of regularity for the coefficient functions β_j^* . Second, it results in a spectral decomposition that facilitates the approximation of the objective function within finite-dimensional subspaces. The spaces \mathbb{H} and \mathbb{K} share the same orthonormal basis (given by the eigenfunctions of K), hence they are defined on the same algebraic structure, but the topology of \mathbb{K} is finer and induces a stronger norm than that of \mathbb{H} . This distinction allows us to define the objective function of SOFIA and the following penalized least squares estimator of the coefficients in eq. (1):

$$\hat{\beta} = \underset{\beta \in \mathbb{K}^p}{\operatorname{argmin}} \frac{1}{2n} \sum_{i=1}^n \left(Y_i - \sum_{j=1}^p \langle \beta_j, X_{ij} \rangle_{\mathbb{H}} \right)^2 + \lambda \sum_{j=1}^p \tilde{w}_j \|\beta_j\|_{\mathbb{K}}, \quad (2)$$

where λ is a tuning parameter and \tilde{w}_j are adaptive weights designed to penalize smaller coefficient norms more heavily.

A crucial challenge in functional regression is the infinite-dimensional nature of the problem. This issue is particularly pronounced in scalar-on-function regression, where the empirical covariance matrix contains finite-rank operators on \mathbb{H} and cannot be invertible as an operator. To address this issue, a common approach in the literature is the so-called *sieve method* (Wang et al., 2016), which consists in projecting the predictors onto a finite-dimensional subspace of \mathbb{H} , denoted by $\mathbb{H}^{(m)}$. This subspace is defined by an orthonormal basis, which may be predefined (e.g., splines), data-driven (e.g., functional principal components), or derived from a general basis (Roche, 2023). In the sieve method, the functional entities in the model are approximated over a sequence of nested finite-dimensional subspaces whose union is dense in the underlying Hilbert space. As the sample size increases, the sieve subspace expands, enabling the estimator to approximate the true functional parameters more accurately. This highlights the nonparametric nature of the problem, where consistent estimation is achieved by letting the complexity of the model (the sieve dimension m) grow with the sample size rather than fixing a finite number of parameters. Following this method, we derive the required basis from the eigenfunctions of the operator K , which allows us

to project both functional predictors and coefficient functions onto the subspaces $\mathbb{H}^{(m)}$ and $\mathbb{K}^{(m)}$, respectively, and to obtain the following finite-dimensional approximation of eq. (2) on $\mathbb{K}^{(m)}$:

$$\hat{\beta}^{(m)} = \operatorname{argmin}_{\beta \in \mathbb{K}^{(m)p}} \frac{1}{2n} \sum_{i=1}^n \left(Y_i - \sum_{j=1}^p \langle \beta_j, X_{ij}^{(m)} \rangle_{\mathbb{H}} \right)^2 + \lambda \sum_{j=1}^p \tilde{w}_j \|\beta_j\|_{\mathbb{K}}. \quad (3)$$

1.1 Related works

The problem of variable selection for scalar-on-function regression models with multiple functional predictors was first examined by Cardot et al. (2007), which employed best subset selection in the context of ozone prediction. Although a few methods have been proposed since then, the literature on the subject remains relatively limited. Most of these existing methods are based on a group modeling strategy (Aneiros et al., 2022) which allows replacing functional variables with a group of scalar variables, and hence reformulating the model as a multiple regression model with grouped predictors. Briefly, each functional variable is expanded using a pre-defined basis system (e.g., B-splines or Fourier basis) and the expansion is then truncated to obtain a finite-dimensional representation of the variable. A grouped variable selection method (see, e.g., Yuan and Lin, 2006) is then employed to select groups of predictors, which correspond to functional variables. The first two works proposing this strategy are Matsui and Konishi (2011), which use Gaussian basis functions combined with a penalized least squares approach, and Gertheiss et al. (2013), which employ B-spline basis functions with an adaptive group lasso penalty for variable selection. In the latter, the penalty includes two components (controlled by two different parameters) to regulate the sparsity of the solution and enforce smoothness, respectively. While these methods are interesting from an algorithmic point of view, they do not provide theoretical guarantees on the selection of the true active variables.

Among the methods based on a group modeling strategy that provide theoretical guarantees on variable selection performance, we find Fan et al. (2015), which use a generic basis and a group lasso penalty, and Lian (2013) and Huang et al. (2016) which expand the functional data through functional principal components (FPCA) and use penalized least squares and penalized least absolute deviation, respectively. In particular, Fan et al. (2015) propose a functional additive regression model that includes linear regression. This study provides a rigorous asymptotic analysis, also when the number of predictors exceeds the sample size. However, the assumption that predictors are known to belong to a Sobolev ellipsoid is quite restrictive. Huang et al. (2016) propose a similar method employing FPCA to expand functional predictors and a different penalty term. While this approach yields similar analytical results, it is more computationally complex, since it requires estimating a set of basis functions for each functional predictor. Finally, Lian (2013) provides asymptotic results in the case of fixed number of predictors and of active predictors. More recently, Boschi et al. (2025) introduced FASTEN, an adaptive elastic net method for variable selection in function-on-function regression, which can be applied also to the scalar-on-function case. This work also expands the functional data using FPCA, and proves an asymptotic oracle property.

All the variable selection methods mentioned above only consider the case of functional data belonging to $L^2(T)$, where T is a bounded interval in \mathbb{R} . To the best of our knowledge, Roche (2023) is the only work considering predictors in general Hilbert spaces and proving asymptotic and non-asymptotic properties. In particular, it proposes two adaptations of the group lasso that satisfy sharp oracle inequalities for prediction errors. However, it does not prove results on the selection of the true active variables nor on the coefficient estimations, which we prove for SOFIA.

RKHS, which play an essential role in our study, have received considerable attention over the past two decades in functional linear regression. A seminal contribution is represented by Yuan and Cai (2010), who introduced a smoothness regularization method based on RKHS. Since then, RKHS-based approaches have been employed in various FDA studies for different purposes. For the foundational aspects of RKHS in functional regression models, we refer to Kadri et al. (2010); recent advancements can be found in Wang et al. (2022). In the context of RKHS-based linear regression, two approaches can be used for parameter estimation, namely the *representer theorem* and *functional subgradients*. The former is the dominant approach in the literature due to its theoretical convenience (see, e.g., Yuan and Cai, 2010; Shin and Lee, 2016; Berrendero et al., 2019). However, the methods based on the representer theorem tend to be computationally slow (Parodi and Reimherr, 2018). For this reason, SOFIA is based on functional subgradients (Bauschke et al., 2011, Chapter 16).

Finally, SOFIA takes inspiration from a series of papers by Reimherr and coauthors on variable selection based on lasso regularization. While these papers explore function-on-scalar regression as opposed to scalar-on-function regression, we borrow from them the definition of functional oracle property and of the Hilbert space \mathbb{K} . Barber et al. (2017) propose FS-Lasso, a method based on the (unweighted) group lasso. Although the oracle property is not satisfied, they give some reasonable bounds for estimation and prediction errors. Fan and Reimherr (2017) propose an adaptive version of the penalty term in Barber et al. (2017) and prove the (functional) oracle property of the resulting method. Finally, FLAME (Parodi and Reimherr, 2018) satisfies the oracle property for variable selection, while ensuring desired properties such as smoothness or periodicity for the coefficients by requiring that they belong to an RKHS.

1.2 Our contributions

The general objective of this paper is to introduce a method for variable selection in scalar-on-function regression models that ensures the regularity of the estimated coefficients while satisfying the functional oracle property.

Our first theoretical result concerns the estimator of eq. (3) in the (non-adaptive) case of $\tilde{w}_j = 1$ and states that, under a suitable restricted eigenvalue (RE) condition, the estimation error admits a sharp bound. Although Barber et al. (2017) established a similar result, we provide a novel proof for predictors that are finite-dimensional truncations of functional data, i.e. vectors. Our main theorem (i.e., Theorem 2) proves the functional oracle property of SOFIA in the spirit of Fan and Reimherr (2017). That is, SOFIA correctly identifies the true predictors with probability tending to one as the sample size n increases, under some appropriate assumptions on the finite-dimensional projections. If the tails of the true coefficients after truncation decay rapidly, then the estimation error declines with the nonparametric rate $o_P(\tau_m/n^{1/2})$, where τ_m is the minimum eigenvalue of the empirical covariance in $\mathbb{K}^{(m)}$. Importantly, this result also holds in the topology of \mathbb{H} . This responds to an open question of Parodi and Reimherr (2018).

Another major contribution is the comparison of the variable selection and estimation performance of multiple recent methods in different simulation scenarios. In particular, we compare SOFIA with the standard group Lasso (Fan et al., 2015), the semi-adaptive and adaptive group Lasso (Gertheiss et al., 2013), the method of Roche (2023), and FAStEN (Boschi et al., 2025).

Finally, we provide a real-world example for predicting Canadian GDP growth using several economic and financial variables. This application presents several challenges, such as handling unbalanced data and high-frequency variables, which we address by representing the predictors as functional objects.

1.3 Organization of paper

Section 2 introduces the framework and assumptions about the data and coefficients, and provides the mathematical notation and technical conditions needed for the theoretical analysis. Section 3 presents the main theoretical results. Section 4 details the implementation procedure based on functional subgradients. Section 5 presents an extensive simulation study and compares SOFIA’s performance with existing approaches. Section 6 provides a real-data application to the prediction of GDP growth. Finally, Section 7 concludes the work.

2 Mathematical framework

In this section, we describe the general structure of the Hilbert space in which the functional predictors are defined and present the model assumptions, including regularity conditions on the coefficient functions and the structure of the trace-class operator that defines the Hilbert subspace where the coefficients reside. We then provide a structured set of assumptions that ensure the uniform convergence of the estimation procedure.

We assume that the predictors X_{ij} are elements of real separable Hilbert space $(\mathbb{H}, \|\cdot\|_{\mathbb{H}})$, where the norm is derived from the inner product $\langle \cdot, \cdot \rangle_{\mathbb{H}}$. Note that \mathbb{H} encompasses a wide range of spaces, including $L^2[0, 1]$ (used in the simulations of Section 5), \mathbb{R}^N , and more specialized function spaces commonly used in statistics, such as product spaces, Sobolev spaces, Wiener spaces, and RKHS.

To ensure regularization of the coefficient functions β_j^* , we follow the approach of Parodi and Reimherr (2018). We consider a (compact) trace-class operator, $K : \mathbb{H} \rightarrow \mathbb{H}$, which is positive definite and self-adjoint. The spectral theorem for compact self-adjoint operators implies that K can be decomposed as $K = \sum_{l=1}^{\infty} \theta_l v_l \otimes v_l$, where $\theta_1 \geq \theta_2 \geq \dots > 0$ are the ordered eigenvalues and $v_l \in \mathbb{H}$ are the corresponding eigenfunctions, which constitute an orthonormal basis for \mathbb{H} (Murphy, 1990, Theorem 2.4.4). The notation $x \otimes y$ denotes the rank-one operator defined by $(x \otimes y)(h) := \langle y, h \rangle_{\mathbb{H}} x$ for any $x, y, h \in \mathbb{H}$. We define the subspace \mathbb{K} of \mathbb{H} as

$$\mathbb{K} := \left\{ h \in \mathbb{H} : \sum_{l=1}^{+\infty} \frac{|\langle h, v_l \rangle_{\mathbb{H}}|^2}{\theta_l} =: \|h\|_{\mathbb{K}}^2 < +\infty \right\}, \quad (4)$$

which is a Hilbert space with norm $\|\cdot\|_{\mathbb{K}}$, \mathbb{K} . When $\mathbb{H} = L^2[0, 1]$, many examples can be found in the literature. In particular, if K is defined as an integral operator associated with a kernel function $k(t, s)$ in a compact domain, then K is a trace-class, positive, and self-adjoint operator. As a result, any RKHS can be viewed as a special case of \mathbb{K} . For a detailed discussion on compact and trace-class operators in Hilbert spaces, we refer to Murphy (1990), Section 2.4. For an overview of various types of kernel, see Berlinet and Thomas-Agnan (2011), Chapter 7. We assume that the coefficient functions β_j^* belong to \mathbb{K} , ensuring the desired level of regularity of the coefficients by choosing an appropriate operator K . The objective function of SOFIA, shown in eq. (2), utilizes the \mathbb{K} -norm in the penalty term, while the least squares term involves the inner product in \mathbb{H} . We study the relationship between \mathbb{K} and \mathbb{H} in Subsection S1.1 of the Supplementary material. Intuitively, we show that \mathbb{K} is the range of the operator $K^{1/2}$, with an appropriate topology, and its norm can be characterized by $\|x\|_{\mathbb{H}} = \|K^{1/2}(x)\|_{\mathbb{K}}$. We also show that \mathbb{K} is dense in \mathbb{H} under the norm of \mathbb{H} .

2.1 Model

The following assumption establishes the foundational framework for our functional linear model by specifying the structure of the response, the predictors, and the coefficient functions.

Assumption 1. Let Y_i denote the scalar response for subject i , and $X_i = (X_{i1}, \dots, X_{ip}) \in \mathbb{H}^p$ represent the deterministic functional predictors. Without loss of generality, we assume that Y_i is centered and the predictors standardized, i.e., $\sum_{i=1}^n Y_i = 0$, $\sum_{i=1}^n X_{ij} = 0$, and $n^{-1} \sum_{i=1}^n \|X_{ij}\|_{\mathbb{H}}^2 = 1$, $j = 1, \dots, p$. We assume that they satisfy the functional linear model of eq. (1) with coefficient functions $\beta^* = (\beta_1^*, \dots, \beta_p^*) \in \mathbb{K}^p \subset \mathbb{H}^p$. The errors ε_i are i.i.d. random variables with mean zero and variance σ^2 . In addition, for constants $C_1, C_2 > 0$, we assume that $P\{|\varepsilon_i| > t\} \leq C_1 \exp(-C_2 t^2)$ for all $t \geq 0$ and $i = 1, 2, \dots, n$.

Moreover, we assume that only the first $p_0 < p$ predictors are active, while the remaining $p - p_0$ predictors do not contribute to Y_i . Consequently, their corresponding coefficients are zero.

We note that the sub-Gaussian tail condition on the errors is satisfied, for instance, by Gaussian random variables (Boucheron et al., 2013, Section 2.3). Importantly, in our model the number of predictors p and the number of active predictors p_0 are not fixed, but can increase with the sample size n . In particular, we require p_0 to be much smaller than both n and p , while we allow p to grow even exponentially with n in our asymptotic results.

2.2 Finite-dimensional approximation

In infinite-dimensional Hilbert spaces, the covariance operator is typically non-invertible due to its finite rank. To address this issue, we restrict the covariance operators to finite-dimensional subspaces of \mathbb{K} . In particular, the *sieve method* (Wang et al., 2016) enables us to approximate our infinite-dimensional estimator of eq. (2) by solving a sequence of finite-dimensional problems. Following Fan et al. (2015), we consider a sequence of integers $m = m_n = O(n)$, which depends only on the sample size n . As n grows to infinity, the dimension m also tends to infinity and the sieve subspaces become dense in \mathbb{K} , allowing the estimator to converge to the true coefficient functions. Let $\mathbb{K}^{(m)}$ denote the m -dimensional subspace of \mathbb{K} spanned by $\{v_1, \dots, v_m\}$, and $\mathbb{K}^{(m)\perp}$ its orthogonal complement. The projections of $\beta_j \in \mathbb{K}$ on $\mathbb{K}^{(m)}$ and $\mathbb{K}^{(m)\perp}$ are denoted by $\beta_j^{(m)}$ and $\beta_j^{(m)\perp}$, respectively. We use the analogous notation for the projections of X_{ij} onto $\mathbb{H}^{(m)}$ and $\mathbb{H}^{(m)\perp}$.

In order to approximate the functional coefficients and predictors while controlling the approximation errors, we impose standard assumptions on their bounds.

Assumption 2. There exist constants $b_1, b_2 > 0$ and $\gamma > 1$ such that $p_0 = o(m^{(\gamma-1)/2})$, and the active coefficients and predictors satisfy:

$$\|\beta_j^*\|_{\mathbb{K}} \leq b_1 \quad \text{and} \quad \sup_{1 \leq i \leq n} \theta_l \langle X_{ij}, v_l \rangle_{\mathbb{H}}^2 \leq b_2 l^{-\gamma} \quad \text{for all } j = 1, \dots, p_0 \text{ and } l \geq 1.$$

The assumption on the true coefficients implies that such coefficients are uniformly bounded, a standard assumption in infinite-dimensional regression models (Fan et al., 2015). Since we work with deterministic predictors, the condition on the active predictors is satisfied, for example, when $\|X^{[j]}\|_{\mathbb{H}}$, the column of the design matrix related to the j^{th} predictor, is uniformly bounded and the operator K exhibits at least a polynomial decay rate ($\theta_l \leq Cl^{-\gamma}$ for some constants $C > 0$ and $\gamma > 1$). The operator K meets this assumption, for example, when it is induced by the Gaussian kernel

or the Matérn kernels. Indeed, the Gaussian kernel has exponential decay, while the Matérn kernel has a decay rate of the form $\theta_l \leq Cl^{-(1+2\nu)}$ (Widom, 1964), hence the assumption is satisfied for any smoothing parameter $\nu > 0$. A condition similar to the bounded design is used in Roche (2023), where a deterministic design matrix is considered. The condition $p_0 = o(m^{(\gamma-1)/2})$ reflects the fact that we are working in a sparse regime, where the number of active functional predictors grows more slowly than $m^{(\gamma-1)/2}$, where m is the sieve dimension and γ the spectral decay. For kernels with fast spectral decay (e.g., Gaussian kernel or Matérn kernel with $\nu > 1$), this requirement is really mild, whereas for kernels with a slower decay rate, such as exponential/Laplacian kernels, it corresponds to the sparsity condition $p_0 = o(\sqrt{m})$.

The predictors and coefficients can be expanded on the basis $\{v_l\}_{l=1}^{+\infty}$ as

$$X_{ij} = \sum_{l=1}^{+\infty} \langle X_{ij}, v_l \rangle_{\mathbb{H}} v_l, \quad \beta_j^* = \sum_{l=1}^{+\infty} \langle \beta_j^*, v_l \rangle_{\mathbb{H}} v_l.$$

If we restrict the predictors and coefficients to the m -dimensional subspaces, we obtain the following decomposition for our regression model (1):

$$Y_i = \sum_{j=1}^{p_0} \left\langle \beta_j^{*(m)}, X_{ij}^{(m)} \right\rangle_{\mathbb{H}} + \sum_{j=1}^{p_0} e_{ij} + \varepsilon_i, \quad (5)$$

where e_{ij} denotes the approximation error, defined as $e_{ij} = \sum_{l=m+1}^{\infty} \langle X_{ij}, v_l \rangle_{\mathbb{H}} \langle \beta_j^*, v_l \rangle_{\mathbb{H}}$. Proposition S2 of Subsection S1.2 of the Supplementary material shows that, under Assumption 2, these approximation errors converge uniformly to zero as $m \rightarrow +\infty$. This permits us to consider the finite-dimensional truncation of model (1):

$$Y_i = \sum_{j=1}^{p_0} \left\langle \beta_j^{*(m)}, X_{ij}^{(m)} \right\rangle_{\mathbb{H}} + \varepsilon_i. \quad (6)$$

To estimate the finite-dimensional coefficients, we consider the objective function of SOFIA:

$$L_\lambda : \mathbb{K}^{(m)} \longrightarrow \mathbb{R}^+, \quad L_\lambda(\boldsymbol{\beta}) = \frac{1}{2n} \sum_{i=1}^n \left(Y_i - \sum_{j=1}^p \left\langle \beta_j, X_{ij}^{(m)} \right\rangle_{\mathbb{H}} \right)^2 + \lambda \sum_{j=1}^p \tilde{w}_j \|\beta_j\|_{\mathbb{K}}. \quad (7)$$

The weights \tilde{w}_j are chosen adaptively. First, we set all weights to 1 to perform an initial selection and obtain an estimate $\tilde{\beta}_j$. Second, we perform an adaptive step with weights $\tilde{w}_j = 1/\|\tilde{\beta}_j\|_{\mathbb{K}}$.

Next, we introduce some notation. We use bold symbols to denote vectors and matrices. Let $\mathbf{X} = (X_{ij}) \in \mathbb{H}^{n \times p}$ be the Hilbert-valued deterministic design matrix, which we partition as $\mathbf{X} = (\mathbf{X}_1, \mathbf{X}_2)$, where $\mathbf{X}_1 \in \mathbb{H}^{n \times p_0}$ and $\mathbf{X}_2 \in \mathbb{H}^{n \times (p-p_0)}$ represent the submatrices of active and null predictors, respectively. The support of $\boldsymbol{\beta}^*$ is defined as $\mathcal{A} = \{1, \dots, p_0\}$ and its complement is \mathcal{A}^c . When there is no ambiguity, we denote the inner product and norm of both \mathbb{K}^p and \mathbb{K} using the same notation.

Since the least squares estimator is based on the inner product of \mathbb{K} , we define the covariance operator between two predictors as an operator on \mathbb{K} . For $j, k = 1, \dots, p_0$, the empirical covariance operators are

$$\hat{\Gamma}_{jk} : \mathbb{K} \longrightarrow \mathbb{K}, \quad \hat{\Gamma}_{jk}(h) = \frac{1}{n} \sum_{i=1}^n \langle h, K(X_{ik}) \rangle_{\mathbb{K}} K(X_{ij}). \quad (8)$$

These operators incorporate the projection of predictors in the range of K . In addition, we define the Hilbert-valued cross-covariance for $j = 1, \dots, p_0$ as

$$\hat{\Gamma}_{YX_j} = \frac{1}{n} \sum_{i=1}^n Y_i K(X_{ij}) \in \mathbb{K}.$$

We denote by $\hat{\Gamma}_{\mathbf{X}_1}$ the $p_0 \times p_0$ matrix of operators $\hat{\Gamma}_{jk}$ and define the vector of cross-covariance operators as $\hat{\Gamma}_{Y\mathbf{X}_1} = (\hat{\Gamma}_{YX_1}, \dots, \hat{\Gamma}_{YX_{p_0}})^\top$. The cross-covariance operator-valued matrix between null and active predictors is denoted by $\hat{\Gamma}_{\mathbf{X}_2\mathbf{X}_1}$ and is defined analogously. For $j, k = 1, \dots, p$, the finite-dimensional covariance operators, indicated by $^{(m)}$, are

$$\hat{\Gamma}_{jk}^{(m)} : \mathbb{K}^{(m)} \longrightarrow \mathbb{K}^{(m)}, \quad \hat{\Gamma}_{jk}^{(m)}(h) = \frac{1}{n} \sum_{i=1}^n \left\langle h, K(X_{ik}^{(m)}) \right\rangle_{\mathbb{K}} K(X_{ij}^{(m)}).$$

Finally, we focus on the oracle estimator. This estimator, denoted by $\hat{\beta}^O = (\hat{\beta}_1^O, \dots, \hat{\beta}_p^O)$, is typically defined as the least squares estimator for active predictors, while it is set to zero for inactive ones. However, in scalar-on-function regression, the empirical covariance matrix $\hat{\Gamma}_{\mathbf{X}_1}$ is always singular, making the least squares estimator inaccessible. In our theory, we work on finite-dimensional spaces $\mathbb{K}^{(m)}$ and define the sieve-oracle estimator as $\hat{\beta}_1^{O(m)} = (\hat{\beta}_1^{O(m)}, 0)$ where $\hat{\beta}_1^{O(m)} = \hat{\Gamma}_{\mathbf{X}_1}^{(m)-1} \hat{\Gamma}_{Y\mathbf{X}_1}^{(m)}$. In Section 3, we demonstrate that our estimator satisfies the functional oracle property. Then, we show that under appropriate assumptions, it tends to the true beta at a rate determined by the minimum eigenvalue of the empirical covariance matrix. For more information on the oracle estimator and the functional oracle property, see, for example, Fan and Reimherr (2017).

2.3 Restricted eigenvalue (RE) condition

In our approach, as a first step, we set all the weights in the objective function (7) to 1. The obtained estimator does not achieve the oracle property, similar to the scalar case (Fan and Li, 2001). Nevertheless, in Theorem 1, we show that under an appropriate version of the RE condition, a tight bound can be found for the distance between the true and the estimated coefficients. We use this bound in the adaptive step to prove the oracle property.

When the predictors are functional, the classic definition of the RE condition is never met: when the dimension of the underlying space is infinity, the lower bound in the RE condition is always zero (Roche, 2023, Lemma 2.1). To overcome this issue, Roche (2023) proposes to define the RE condition through a sequence $\alpha_n^{(m)}$ of nonnegative (possibly zero) values. We adopt a similar approach and consider the following condition.

Assumption 3. (RE condition) For the dimension m , there exists a positive number α_m such that

$$\alpha_m := \min \left\{ \frac{\left\| \Gamma_{\mathbf{X}\mathbf{X}}^{(m)1/2} \boldsymbol{\delta} \right\|_{\mathbb{K}}}{\left\| \boldsymbol{\delta} \right\|_{\mathbb{K}}} : |J| \leq p_0, \boldsymbol{\delta} = (\delta_1, \dots, \delta_p) \in \mathbb{K}^{(m)} \setminus \{0\}, \left\| \boldsymbol{\delta}_{J^c} \right\|_{\ell_1/\mathbb{K}} \leq 3 \left\| \boldsymbol{\delta}_J \right\|_{\ell_1/\mathbb{K}} \right\},$$

where $\left\| \boldsymbol{\delta} \right\|_{\mathbb{K}} = \left(\sum_{j=1}^p \left\| \delta_j \right\|_{\mathbb{K}}^2 \right)^{1/2}$ represents the ℓ_2 norm, $\left\| \boldsymbol{\delta}_J \right\|_{\ell_1/\mathbb{K}} = \sum_{j \in J} \left\| \delta_j \right\|_{\mathbb{K}}$ and J^c denotes the complement of the set J .

Note that our RE condition differs from that of Roche (2023) in two key aspects. First, in our definition, we construct the covariance operators using the approximated predictors instead of the predictors. Second, we assume that the dimension m depends on the sample size n and is smaller than it, while Roche (2023) treats the dimension m and the sample size n as independent, allowing m to grow to infinity while n remains fixed. As a result, in Roche (2023) for sufficiently large dimensions $\alpha_n^{(m)}$ can become zero. In contrast, in our setting m depends on n , and $m = O(n)$. In this way, the lower bounds $\alpha^{(m)}$ in Assumption 3 can form a sequence of strictly positive scalars, typically tending to zero. For more details on the RE condition, see Bickel et al. (2009) for lasso, Lounici et al. (2011) for group lasso, Bellec and Tsybakov (2017) for a general convex penalty, and Barber et al. (2017) for function-on-scalar models.

2.4 Asymptotic assumptions

We use the following technical assumptions, which are well-documented in the literature, to assess the asymptotic behavior of our model. If the design matrix is scalar-valued, the upper and lower bounds are typically assumed to be constant (see Huang et al., 2008; Fan and Reimherr, 2017; Parodi and Reimherr, 2018; Mirshani and Reimherr, 2021). In contrast, following Roche (2023), we assume that these bounds are sequences that tend to zero as m increases. We study the relation between the RE condition and Assumption 4 in Proposition S3 in Subsection S1.3 of the Supplementary material. Specifically, we show that when the covariance between the null predictors tends to zero rapidly, the RE condition is met under Assumption 4.

Assumption 4. *For the dimension m , the following conditions hold.*

1. Let σ_{\min} and σ_{\max} be the smallest and largest eigenvalues of $\hat{\Gamma}_{\mathbf{X}_1}^{(m)}$, respectively. There exist a fixed constant τ and a sequence $\tau_m > 0$ such that

$$\frac{1}{\tau_m} \leq \sigma_{\min} \left(\hat{\Gamma}_{\mathbf{X}_1}^{(m)} \right) \leq \sigma_{\max} \left(\hat{\Gamma}_{\mathbf{X}_1}^{(m)} \right) \leq \tau.$$

2. Let $b = \min_{j \in \mathcal{A}} \|\beta_j^*\|_{\mathbb{K}}$, $b_m = \min_{j \in \mathcal{A}^{(m)}} \|\beta_j^{*(m)}\|_{\mathbb{K}}$, and $\zeta_m = \min\{\tau_m^{-1}, \alpha_m^2\}$. Then,

$$\max_{j \in \mathcal{A}} \|\beta_j^* - \beta_j^{*(m)}\|_{\mathbb{K}} = o(b), \quad \text{and} \quad b_m \gg p_0 \sqrt{\log(p)} / \zeta_m \sqrt{n}.$$

3. The tuning parameter λ satisfies the bounds $p_0^{1/2} \log(p) \zeta_m^{-1} n^{-1} \ll \lambda \ll b_m p_0^{-1/2} n^{-1/2}$.

4. Let $\|\cdot\|_{op}$ denote the operator norm. Then, $\|\hat{\Gamma}_{\mathbf{X}_2 \mathbf{X}_1}^{(m)} \hat{\Gamma}_{\mathbf{X}_1}^{(m)-1}\|_{op} = \varphi_m < 1$.

These assumptions are counterparts to some standard assumptions in the high-dimensional regression literature. The first one, often called *design matrix condition* in the scalar design, ensures that the true predictors exhibit regular behavior and are not excessively correlated. This condition is imposed by setting fixed lower and upper bounds for the eigenvalues. In our approach, since $\hat{\Gamma}_{\mathbf{X}_1}$ is a finite-rank operator on an infinite-dimensional Hilbert space \mathbb{H}^{p_0} , it is never injective, and so 0 is always an eigenvalue. To address this issue, we restrict our analysis to finite-dimensional subspaces of the underlying infinite-dimensional space, making it natural to impose a sequence of bounds that depend on both the dimension and the sample size. Typically, $(\tau_m)^{-1}$ has zero as an accumulation point, since, as the sample size increases, $\hat{\Gamma}_{\mathbf{X}_1}^{(m)}$ converges to a compact operator (not necessarily of

finite rank), and compact operators usually have 0 as a limit point of their eigenvalues (unless they are of finite rank). This implies that the design matrix becomes increasingly ill-conditioned and nearly singular as n grows. This ill-posedness is controlled by the assumptions on the minimum norm of the coefficients and the tuning parameter. In contrast, when the population covariance $\Gamma_{\mathbf{X}_1}$ is bounded, the upper eigenvalue bound can be taken as fixed, similar to scalar cases. The second group of conditions corresponds to the *minimum signal condition*. It plays two roles in our study. First, it ensures that sieve truncation does not erase the active coefficients. Second, it allows the smallest β_j^* to vary with the sample size, dimension, lower bound of the eigenvalues, and RE bound, while ensuring that it does not become too small. If $(\tau_m)^{-1}$ or α_m^2 decay too rapidly in relation to sample size, number of predictors, and number of active predictors, then there is no guaranty that the model is able to select predictors with small norms. The third condition prevents the tuning parameter from growing too rapidly or too slowly as n grows. The lower bound prevents overfitting by controlling false positives, while the upper bound ensures that relevant predictors are not excessively penalized, avoiding false negatives. Finally, the fourth condition, known as the *irrepresentable condition*, ensures that the true and the null predictors do not exhibit a high correlation. In the literature on scalar predictors, the sequence φ_m is supposed to be a fixed number, usually lower than 1. This requirement has been established as a necessary condition for having the oracle property: see, e.g., (see, e.g., Zhao and Yu, 2006, for formal definitions and proofs).

3 Theoretical results

This section presents the theoretical results of the paper. We begin with a concentration inequality that bounds the tail probability of a weighted sum of Hilbert space-valued random variables and serves as a key component in the proofs of Theorems 1 and 2. This result is an extension of Lemma 1 in the supplementary material of Huang et al. (2008) to the Hilbert space setting. Its proof is given in Subsection S1.4 of the Supplementary material.

Lemma 1 (Hilbert-valued concentration inequality). *Let $\mathbf{X} = (X_{ij}) \in \mathbb{H}^{n \times p}$ and $\varepsilon = (\varepsilon_1, \dots, \varepsilon_n)$ be as in Assumption 1. For each $j = 1, \dots, p$, define $Z_j := n^{-1} \sum_{i=1}^n \varepsilon_i X_{ij}$. Then, for any $t > 0$,*

$$P(\|Z_j\|_{\mathbb{H}} > t) \leq \exp\left(-\frac{nt^2}{M}\right),$$

where $M > 0$ is a constant depending only on the constants C_1 and C_2 in Assumption 1.

The following theorem provides the bounds for the estimation and prediction errors of the unweighted scalar-on-function lasso. A similar theorem for classic multiple regression can be found in Chapter 6 of Bühlmann and Van De Geer (2011). The function-on-scalar case is proved in Barber et al. (2017). Our contribution is two-fold. First, we design a concentration inequality for Hilbert-valued design matrices. Then, we develop the estimation and error analysis in a separable Hilbert space. The non-asymptotic and asymptotic convergence rates are nonparametric counterparts of those of the scalar case. This is because our Hilbert-valued concentration inequality mirrors the scalar structure. These rates are crucially dependent on the sequence $\{\alpha_m\}_{m \in \mathbb{N}}$ in Assumption 3. This sequence is supposed to be fixed in classic regression models, so it does not have any impact when the sample size increases. However, in the presence of functional predictors, this sequence always tends to zero and its behavior affects the convergence rate of the estimator.

Theorem 1. *Let Assumptions 1-3 hold. Let $\tilde{\beta}^{(m)}$ be any minimizer of the lasso function (7) with weights equal to 1. Let $\delta \in (0, 1)$ and $\lambda \geq 2\sqrt{n^{-1}\theta_1 M \log(p/\delta)}$, where $M > 0$ is the constant in Lemma 1. Then,*

$$P\left(\left\|\Gamma_{\mathbf{X}\mathbf{X}}^{(m)1/2}\left(\tilde{\beta}^{(m)} - \beta^{*(m)}\right)\right\|_{\mathbb{K}} \leq \frac{4\lambda\sqrt{p_0}}{\alpha_m}\right) \geq 1 - \delta$$

and

$$P\left(\left\|\tilde{\beta}^{(m)} - \beta^{*(m)}\right\|_{\ell_1/\mathbb{K}} \leq \frac{8\lambda p_0}{\alpha_m^2}\right) \geq 1 - \delta.$$

The proof of Theorem 1 is provided in Subsection S1.5 of the Supplementary material. Its usefulness is apparent in Corollary 1, which is a direct result of Theorem 1 and makes (unweighted) lasso a very good starting point for the adaptive model. In this corollary, the upper bounds are selected in a way that is consistent with the literature (Lounici et al., 2011; Barber et al., 2017; Fan and Reimherr, 2017; Parodi and Reimherr, 2018).

Corollary 1. *Let Assumptions 1-3 hold, and λ decays with rate $\lambda \sim \sqrt{\log(p)/p_0 n}$. Then, for any minimizer $\tilde{\beta}^{(m)}$ of the lasso function (7) with weights equal to 1, for $n \rightarrow +\infty$,*

$$\sup_{j \in \mathcal{A}^{(m)}} \left\|\tilde{\beta}_j^{(m)} - \beta_j^{*(m)}\right\|_{\mathbb{K}} = O_P(\sqrt{r_m}) \quad \text{with} \quad r_m := \frac{p_0 \log p}{\alpha_m^4 n}.$$

We are now in a position to state our main result. We show that, when the sample size grows, SOFIA selects the true predictors and converges to the oracle estimator with probability tending to 1. The proof is provided in Subsection S1.7 of the Supplementary material.

Theorem 2 (Functional oracle property). *Let Assumptions 1-4 hold. For $j = 1, \dots, p$ let $\tilde{\beta}_j^{(m)}$ be the estimator of Theorem 1 and $\hat{\beta}_j^{(m)}$ a minimizer of the function (7) with weights $\tilde{w}_j = \|\tilde{\beta}_j^{(m)}\|_{\mathbb{K}}^{-1}$. Then, when $n \rightarrow +\infty$,*

$$(i) \ P\left(\hat{\mathcal{A}}^{(m)} = \mathcal{A}\right) \rightarrow 1.$$

$$(ii) \ \left\|\hat{\beta}^{(m)} - \hat{\beta}^{O(m)}\right\|_{\mathbb{K}} = o_P(\tau_m/\sqrt{n}).$$

$$(iii) \ \text{If, in addition, } \max_{j \in \mathcal{A}} \|\beta_j^{*(m)\perp}\|_{\mathbb{K}} = o(\tau_m/\sqrt{p_0 n}), \text{ then, as } n \rightarrow +\infty,$$

$$\left\|\hat{\beta}^{(m)} - \beta^*\right\|_{\mathbb{K}} = o_P(\tau_m/\sqrt{n}).$$

The first part of the theorem establishes that SOFIA recovers the true support on the (m) -dimensional subspace, with probability tending to one. This ensures consistent variable selection in the high-dimensional functional setting. The second part shows that SOFIA is equivalent to the oracle estimator in the finite-dimensional space $\mathbb{K}^{(m)}$. This means that SOFIA is asymptotically equivalent to the oracle estimator on $\mathbb{K}^{(m)}$. The third part claims that, if the tails of the projections of β_j^* in $\mathbb{K}^{(m)}$ decay sufficiently fast, then the finite-dimensional lasso estimator converges to β^* in the strong topology of \mathbb{K} . As a result, SOFIA achieves full consistency in \mathbb{K} , under appropriate conditions, despite operating through finite-dimensional approximations. The proof of Theorem 2, inspired by Huang et al. (2008) and Parodi and Reimherr (2018), relies on the functional subgradient of the objective function, together with a concentration inequality for sums of Hilbert-valued random elements. The latter yields high-probability bounds for the stochastic error term. Such bounds are then combined with the adaptive penalization framework to establish both support recovery and estimation consistency.

4 Implementation

To implement SOFIA, we take inspiration from the FLAME method of Parodi and Reimherr (2018) for the function-on-scalar regression case. To find the minimizers of the objective function (7), we propose a coordinate descent algorithm based on the functional subgradient (Bauschke et al., 2011, Chapter 16). In Subsection S1.6 of the Supplementary material we show that, for $j = 1, \dots, p$, the functional subgradient of the function (7) in $\mathbb{K}^{(m)}$ is

$$\begin{aligned} \frac{\partial}{\partial \beta_j} L_\lambda(\boldsymbol{\beta}) &= -\frac{1}{n} \left(\sum_{i=1}^n \left(Y_i - \sum_{k=1}^p \langle \beta_k, K(X_{ik}^{(m)}) \rangle_{\mathbb{K}} \right) K(X_{ij}^{(m)}) \right) \\ &\quad + \lambda \tilde{w}_j \begin{cases} \|\beta_j\|_{\mathbb{K}}^{-1} \beta_j & \text{if } \beta_j \neq 0, \\ \{h \in \mathbb{K}^{(m)} : \|h\|_{\mathbb{K}} \leq 1\} & \text{if } \beta_j = 0. \end{cases} \end{aligned}$$

To update the j^{th} coordinate, we set $\check{\beta}_j = n^{-1} \sum_{i=1}^n (Y_i - \sum_{k \neq j} \langle \hat{\beta}_{k,i}^{[t-1]}, K(X_{ik}^{(m)}) \rangle_{\mathbb{K}}) K(X_{ij}^{(m)})$, where $\hat{\beta}_{k,i}^{[t-1]}$ are the estimates obtained in the previous iteration, and fix the other coordinates. Then, we can separate the contribution of the j^{th} predictor and write

$$\frac{\partial}{\partial \beta_j} L_\lambda(\boldsymbol{\beta}) = -\check{\beta}_j + \hat{\Gamma}_{jj}^{(m)}(\beta_j) + \lambda \tilde{w}_j \begin{cases} \|\beta_j\|_{\mathbb{K}}^{-1} \beta_j & \text{if } \beta_j \neq 0, \\ \{h \in \mathbb{K}^{(m)} : \|h\|_{\mathbb{K}} \leq 1\} & \text{if } \beta_j = 0. \end{cases}$$

Only for implementation, we assume that $\hat{\Gamma}_{jj}^{(m)}$ is equal to the identity matrix. This is equivalent to a well-known *group-wise orthonormality condition* in the group lasso (Roche, 2023). We then set the last equation to zero to find the minimum of $L_\lambda(\boldsymbol{\beta})$, obtaining

$$\hat{\beta}_j = \begin{cases} 0 & \text{if } \|\check{\beta}_j\|_{\mathbb{K}} \leq \lambda \tilde{w}_j, \\ \left(1 + (\lambda \tilde{w}_j) \|\hat{\beta}_j\|_{\mathbb{K}}^{-1}\right)^{-1} \check{\beta}_j & \text{if } \|\check{\beta}_j\|_{\mathbb{K}} > \lambda \tilde{w}_j. \end{cases} \quad (9)$$

The first case in eq. (9) provides an upper bound for λ . If $\lambda \geq (\tilde{w}_j n)^{-1} \|\sum_{i=1}^n Y_i K(X_{ij}^{(m)})\|_{\mathbb{K}}$ for all $j = 1, \dots, p$, then all predictors are discarded. Therefore, to select the grid of λ , we start with this value and decrease it in logarithmically spaced intervals at a prespecified rate until we reach the desired number of values for λ . The second case in eq. (9) enables us to update non-zero coefficients. For $\hat{\beta}_j \neq 0$, we have

$$\hat{\beta}_j = \left(1 + \frac{(\lambda \tilde{w}_j)}{\|\hat{\beta}_j\|_{\mathbb{K}}}\right)^{-1} \check{\beta}_j.$$

This equation does not have a closed form, even for the scalar design. The problem is that the norm of $\hat{\beta}_j$ on the right-hand side is unknown. To overcome this issue, we compute the \mathbb{K} -norm and apply Parseval's identity:

$$\|\hat{\beta}_j\|_{\mathbb{K}}^2 = \sum_{l=1}^m \left\langle \left(1 + \frac{\lambda \tilde{w}_j}{\|\hat{\beta}_j\|_{\mathbb{K}}}\right)^{-1} \check{\beta}_j, v_l \right\rangle_{\mathbb{K}}^2 = \left(1 + \frac{\lambda \tilde{w}_j}{\|\hat{\beta}_j\|_{\mathbb{K}}}\right)^{-2} \sum_{l=1}^m \langle \check{\beta}_j, v_l \rangle_{\mathbb{K}}^2.$$

After some simplifications, we obtain the equation

$$1 = \frac{\sum_{l=1}^m \langle \check{\beta}_j, v_l \rangle_{\mathbb{K}}^2}{\left(\|\hat{\beta}_j\|_{\mathbb{K}} + \lambda \tilde{w}_j \right)^2}.$$

We use the `NLOPT_LN_COBYLA` algorithm from the `R` package `nloptr` to solve this nonlinear equation for $\|\hat{\beta}_j\|_{\mathbb{K}}$. Then, we use a coordinate descent algorithm to iteratively compute estimates $\hat{\beta}^{[t]}$ for $t = 1, 2, \dots$ that converge to $\hat{\beta}$. The iterative algorithm stops when the improvement in the \mathbb{K} -norm of the estimate of β^* reaches a pre-specified threshold. In particular, as stopping criteria, we use a maximum number of iterations of the nonlinear algorithm, a threshold on the improvement of the estimation error, and a kill switch, which means that the process stops when the number of selected variables exceeds a given number. Finally, we employ 5-fold cross-validation to determine the optimal value of λ .

As explained above, we run the algorithm twice. First, we set all the weights \tilde{w}_j to 1 to obtain an initial estimate of the coefficients. Then, for those that have a non-zero norm, we set $\tilde{w}_j = 1/\|\tilde{\beta}_j^{(m)}\|_{\mathbb{K}}$ and run the algorithm a second time to improve the variable selection and refine the estimation.

In the simulation study and real data analysis, we work with the space $\mathbb{H} = L^2$ and assume that K is an integral operator associated with the kernel function $k(t, s)$, i.e., $(Kf)(t) = \int k(t, s)f(s) ds$. The space \mathbb{K} corresponds to the RKHS induced by the kernel function $k(t, s)$. In the literature, two common examples are the Gaussian kernel and the exponential or Laplacian kernel:

$$k_{\infty}(t, s) = \exp\left(\frac{-|t-s|^2}{\rho}\right), \quad k_{1/2}(t, s) = \exp\left(\frac{-|t-s|}{\rho}\right),$$

where the parameter ρ controls the length scale. A lower value of ρ results in a kernel that decays more rapidly as the distance $|t-s|$ increases, leading to functions that exhibit more rapid variations over short distances. The Gaussian kernel $k_{\infty}(t, s)$ is infinitely differentiable and is well suited for modeling very smooth data. The exponential or Laplacian kernel $k_{1/2}(t, s)$ possesses only one continuous derivative, making it more appropriate for modeling rough data. These kernels belong to a broader class known as Matérn kernels, defined by

$$k_{\nu}(t, s) = \frac{2^{1-\nu}}{\Gamma(\nu)} \left(\frac{\sqrt{2\nu}|t-s|}{\rho} \right)^{\nu} K_{\nu} \left(\frac{\sqrt{2\nu}|t-s|}{\rho} \right),$$

where Γ is the Gamma function and K_{ν} denotes the modified Bessel function of the second kind (Genton, 2001). The predictors are expanded on the eigenfunctions of the operator K . To determine the number of basis functions, we use the minimum of n and the smallest number of eigenvalues that satisfy $\sum_{l=1}^m \theta_l \geq 0.99 \sum_{l=1}^{\infty} \theta_l$, which mimics the 99% explanation of data variability in FPCA.

The `R` code implementing SOFIA, as well as an example with simulated data, is provided on the GitHub page <https://github.com/HedayatFathi/SOFIA>.

5 Simulation study

In this section, we conduct a comprehensive simulation study to evaluate SOFIA's performance. We consider both the accuracy of variable selection and the predictive performance in several

scenarios. We generate datasets under different model complexities and signal-to-noise ratios, and compare SOFIA with existing methods under various specifications.

We take the simulation framework from Gertheiss et al. (2013) and introduce some modifications in order to obtain scaled design matrices and curve domain $[0, 1]$. In particular, we set $\mathbb{H} = L^2[0, 1]$ and generate the response according to the model

$$Y_i = \sum_{j=1}^{p_0} \int_0^1 \beta_j(t) X_{ij}(t) dt + \varepsilon_i,$$

where $\varepsilon_i \sim \mathcal{N}(0, \sigma^2)$. The functional predictors are defined as

$$X_{ij}(t) = 0.01 \left(\sum_{r=1}^5 (a_{ijr} \sin(2\pi t(5 - a_{ijr})) - m_{ijr}) + 15 \right),$$

where $i = 1, \dots, n$ denotes the observations, the sample size is fixed to $n = 500$, and the interval $[0, 1]$ is discretized using a grid of 50 equidistant points. The coefficients a_{ijr} and m_{ijr} are independently sampled from the uniform distributions $U(0, 5)$ and $U(0, 2\pi)$, respectively.

The number of predictors p and of active predictors p_0 , indexed by j , vary between the different experimental scenarios. In particular, we consider **high-dimensional** and **moderate** scales, and **very sparse** and **less sparse** regimes for each scale. In the high-dimensional scale, we include $p = 700$ functional predictors, which is particularly challenging due to the large number of features relative to the sample size ($n < p$). Notably, among the competing methods, only FASTEN (Boschi et al., 2025) can handle this setting. In the high-dimensional scale, the very sparse regime considers five active predictors ($p_0 = 5$), while the less sparse regime includes 10 active predictors ($p_0 = 10$). In the moderate scale, the very sparse regime contains $p = 30$ predictors of which $p_0 = 10$ are active, while the less sparse regime has $p = 10$ predictors of which $p_0 = 5$ are active. This moderate scale setting enables broader comparisons across different model complexities with five competing methods. The coefficient functions β_j of the active predictors are simulated based on the Gamma and exponential density functions, as displayed in Figure 1.

For each scenario, we consider five levels of signal-to-noise ratio, namely $\text{SNR} = 0.1, 0.5, 1, 10$, and 100. The variance of the noise term ε_i is set according to the desired SNR level by $\sigma^2 =$

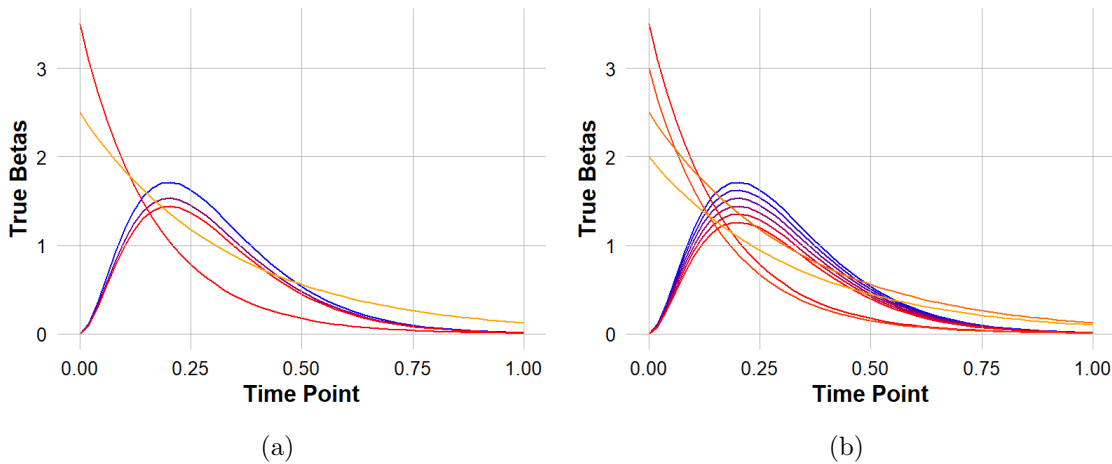


Figure 1: The coefficient functions $\beta_j(t)$ of the active predictors for (a) $p_0 = 5$ and (b) $p_0 = 10$.

$\text{var}(\mathbf{Y}^{true})/SNR$. Here, the noise-free scalar response is defined as $Y_i^{true} = Y_i - \varepsilon_i$, and $\text{var}(\mathbf{Y}^{true})$ denotes its variance over $i = 1, \dots, n$.

The performance of the methods is evaluated based on the average number of true positives (TP) and false positives (FP) across 10 replications. In addition, we assess prediction accuracy by computing the root mean squared error (RMSE) on an independently generated test set of size $n_{\text{test}} = 100$.

To choose the tuning parameter λ in SOFIA, we examine 100 candidate values spaced logarithmically with a ratio of 0.05 (see Section 4), using a 5-fold cross-validation.

5.1 High-dimensional scale

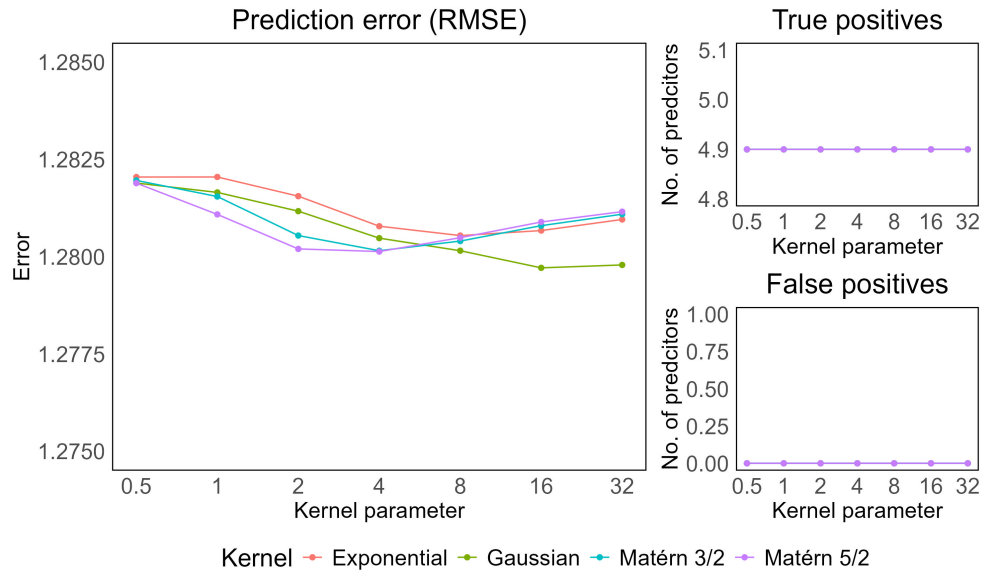
We first compare the performance of SOFIA using different kernel functions (see Section 4) in the high-dimensional scale simulation scenarios, to highlight the impact of the kernel and the choice of the kernel parameter on variable selection and estimation accuracy. In particular, we consider the Gaussian kernel, the exponential kernel, and the Matérn kernels with $\nu = 5/2$ and $\nu = 3/2$ (see Section 4). For these simulations, we set the kill switch, i.e. the maximum number of selected predictors, to $2p_0$.

Figures 2 and 3 display the performance across a range of kernel parameter values for $SNR = 1$ and 10 , respectively, in both regimes. Across all kernels and parameters, SOFIA consistently achieves near-perfect support recovery for both SNR levels. For $SNR = 10$, all kernels perform similarly well, with perfect support recovery (Figure 3). As expected, in the more noisy case ($SNR = 1$) sometimes SOFIA misses an active predictor and/or includes a false positive (Figure 2). For both SNR levels, smoother kernels, especially the Gaussian kernel with high kernel parameters, tend to yield slightly lower RMSE. This behavior is expected, since the simulated data involve smooth coefficient functions and predictors. Results for the high-noise cases ($SNR = 0.1$ and $SNR = 0.5$) and the near-noise-free case ($SNR = 100$) are reported in Subsection S2.1 of the Supplementary material, and show that all kernels and parameters exhibit comparable performance. Importantly, performance in terms of true and false positive is still pretty good in the case of $SNR = 0.5$, while it deteriorates markedly for the very noisy case of $SNR = 0.1$. In Subsection S2.2 of the Supplementary material, we show the estimated coefficient functions $\hat{\beta}$ along with the true β^* in the very sparse regime, for the Gaussian kernel with $\rho = 8$ and for the exponential kernel with $\rho = 2$. The first kernel serves as a reference and provides smooth estimates of the coefficients, while the second one captures less smooth structures. In both cases, SOFIA successfully recovers the overall shape of the true coefficients. The apparent fluctuation of the estimates is primarily controlled by the kernel parameter ρ rather than by the kernel family. A small ρ leads to more local fluctuations, whereas a larger ρ produces smoother estimates.

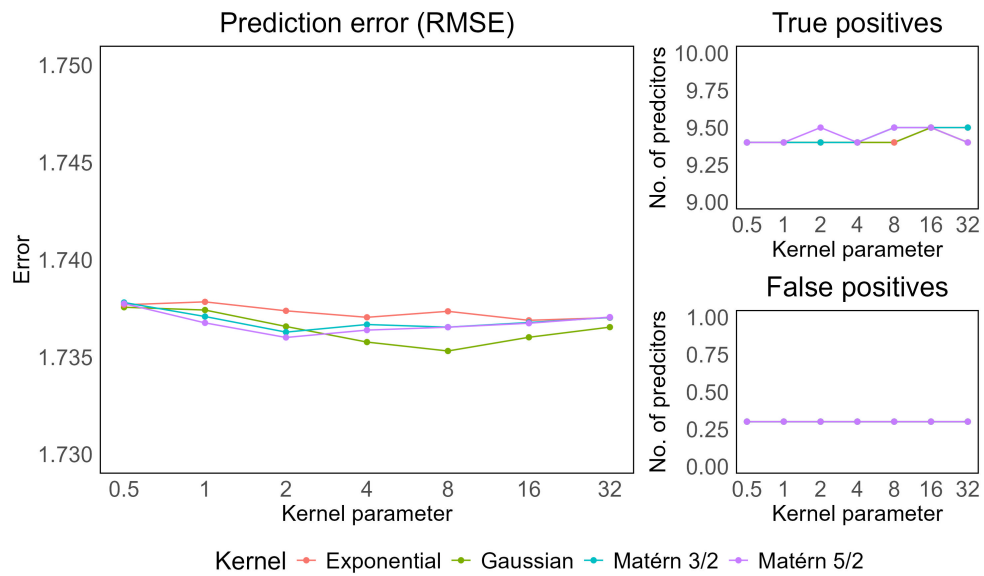
Second, we compare the performance of SOFIA (with Gaussian kernel and $\rho = 8$) and FASStEN (Boschi et al., 2025) across different SNR levels and both sparsity levels. For both methods, we use a kill switch of $2p_0$ predictors. Note that FASStEN is the only competing method that can handle this high-dimensional scale simulation.

Table 1 shows the results of this simulation. For all SNR levels but $SNR = 0.1$, both methods identify all or nearly all true active predictors, with very few false positives. Both methods perfectly recover the true support when the noise is low ($SNR = 100$ and 10). Remarkably, both methods also correctly identify almost all true active predictors, with very few false positives, for $SNR = 1$ and 0.5 . Instead, the case of $SNR = 0.1$ proves to be extremely challenging for both methodologies. Importantly, SOFIA consistently achieves a lower RMSE than FASStEN across all SNR levels, while maintaining strong support recovery. For $SNR = 0.1$ and 0.5 , SOFIA generally recovers more active

SNR = 1



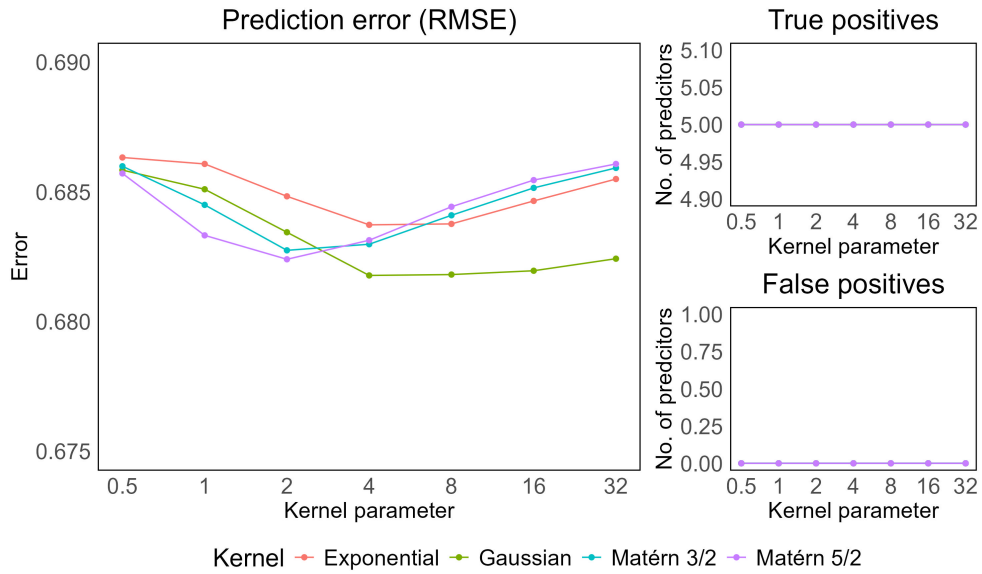
(a) Very sparse regime ($p_0 = 5$).



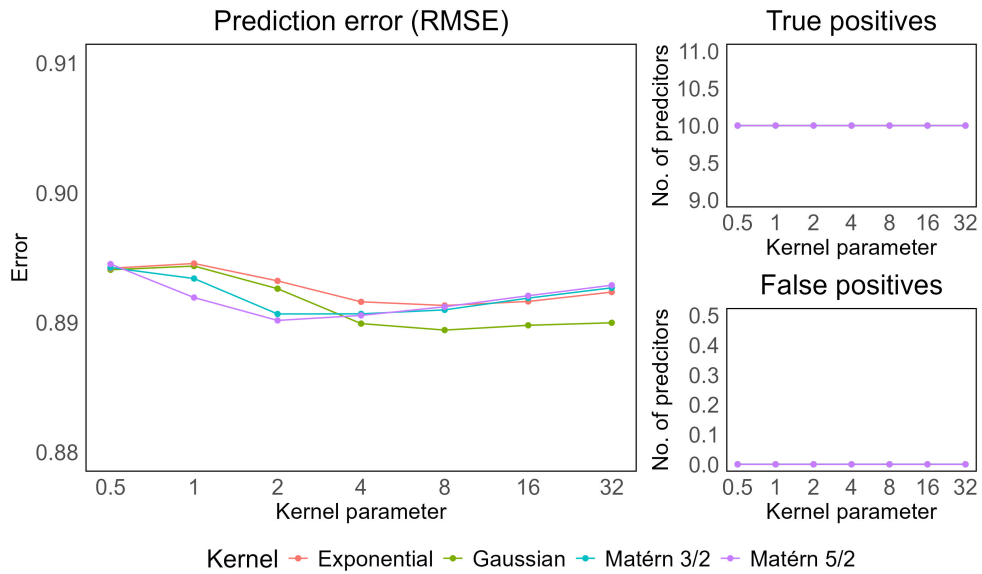
(b) Less sparse regime ($p_0 = 10$).

Figure 2: Comparison of the performance of different kernels under varying parameter values for SNR = 1. Subfigures represent the true positives, false positives, and root mean squared error (RMSE) in the very sparse and less sparse regimes, in the high-dimensional scale ($p = 700$).

SNR = 10



(a) Very sparse regime ($p_0 = 5$).



(b) Less sparse regime ($p_0 = 10$).

Figure 3: Comparison of the performance of different kernels under varying parameter values for SNR = 10. Subfigures represent the true positives, false positives, and root mean squared error (RMSE) in the very sparse and less sparse regimes, in the high-dimensional scale ($p = 700$).

SNR	Method	Very sparse ($p_0 = 5$)			Less sparse ($p_0 = 10$)		
		TP	FP	RMSE	TP	FP	RMSE
0.1	FASTen	1.3	0.8	4.42	0.9	0.6	5.72
	SOFIA	2.3	1.4	3.67	2.1	4.8	4.79
0.5	FASTen	4.9	0.9	2.22	7.8	2.4	2.87
	SOFIA	4.7	0	1.72	8.2	1.5	2.32
1	FASTen	5	0.1	1.75	9.6	1.8	2.28
	SOFIA	4.9	0	1.28	9.4	0.3	1.74
10	FASTen	5	0	1.21	10	0.1	1.60
	SOFIA	5	0	0.68	10	0	0.89
100	FASTen	5	0	1.14	10	0	1.52
	SOFIA	5	0	0.60	10	0	0.73

Table 1: Comparison between SOFIA and FASTen across different SNR levels in the high-dimensional scale ($p = 700$). Bold entries highlight the best-performing method for each metric.

predictors, albeit with slightly higher false positive rate. However, this trade-off results in a better predictive accuracy. At higher SNR levels (SNR = 1, 10, and 100), SOFIA continues to produce a lower RMSE. In general, SOFIA demonstrates superior predictive performance while maintaining competitive (often better) variable selection accuracy.

5.2 Moderate scale

Since most existing methods are computationally infeasible for a large number of predictors and/or cannot handle cases where the number of predictors exceeds the sample size (such as the high-dimensional case shown above), we consider a moderate scale simulation setting to allow for a broader performance comparison. We compare the performance of SOFIA (with Gaussian kernel and $\rho = 8$) with five other methods: the standard non-adaptive group lasso (Fan et al., 2015), adaptive lasso (Adapt1 and Adapt2; Gertheiss et al., 2013), the method of Roche (2023), and FASTen (Boschi et al., 2025). To ensure a fair comparison, all methods are run without a kill switch and with their own default configuration parameters.

Table 2 summarizes the results. In low noise conditions (SNR = 100 and 10), all methods perform generally well. In particular, SOFIA, FASTen, and Roche consistently achieve high true positive recovery with minimal false positives across both regimes. Although standard and adaptive lasso sometimes achieve better RMSE and always select all true active predictors, their elevated false-positive rates make them less suitable for tasks that require precise variable selection and parsimonious models. In high noise conditions (SNR = 0.5 and 1), SOFIA and FASTen effectively balance selection and precision, achieving very high true positive rates with relatively low false positives. In contrast, Roche does not select any feature in these settings (hence showing both 0 true and false positive rates). Both standard and adaptive lasso correctly select all true active predictors but also include several false positives, with Adapt2 performing slightly better than Adapt1 and standard lasso in both regimes. Finally, the very noisy case of SNR = 0.1 is challenging for all methods. However, also in this case SOFIA shows good results both in terms of support

SNR	Method	Very sparse ($p = 30, p_0 = 10$)			Less sparse ($p = 10, p_0 = 5$)		
		TP	FP	RMSE	TP	FP	RMSE
0.1	Standard	8.8	10.1	4.96	5	2.7	3.73
	Adapt1	9.1	10.4	5.23	5	3.2	3.9
	Adapt2	8.8	8.8	5.14	5	2.5	3.77
	Roche	0	0	5.22	0	0	3.86
	FASTen	2.6	0.6	5.77	2.8	0.2	4.50
	SOFIA	6.2	2.3	4.73	4.2	0.4	4.01
0.5	Standard	10	11.3	2.50	5	2.6	1.72
	Adapt1	10	11.5	2.63	5	2.7	1.87
	Adapt2	10	8.8	2.57	5	2	1.77
	Roche	0	0	2.72	0	0	2.02
	FASTen	9.6	1.4	2.93	5	0.2	2.3
	SOFIA	9.7	0.6	2.28	5	0	2.04
1	Standard	10	10.8	1.98	5	2.3	1.26
	Adapt1	10	12.3	2.10	5	2.5	1.41
	Adapt2	10	7.8	2.04	5	1.7	1.31
	Roche	0	0	2.23	0	0	1.65
	FASTen	10	0.5	2.34	5	0.2	1.85
	SOFIA	9.9	0	1.72	5	0	1.57
10	Standard	10	5.9	1.33	5	0.6	0.59
	Adapt1	10	7.4	1.45	5	1.1	0.83
	Adapt2	10	4.6	1.43	5	0.5	0.66
	Roche	9.66	0	1.25	5	0	1.04
	FASTen	10	0.4	1.64	5	0	1.28
	SOFIA	10	0	0.90	5	0	0.92
100	Standard	10	3.4	1.24	5	0.2	0.48
	Adapt1	10	5.1	1.38	5	0.5	0.76
	Adapt2	10	3	1.36	5	0.2	0.54
	Roche	10	0	0.57	5	0	1.00
	FASTen	10	0	1.55	5	0	1.20
	SOFIA	10	0	0.74	5	0	0.79

Table 2: Comparison of SOFIA with five competitor methods across different SNR levels in the moderate scale. Bold entries highlight the best-performing method for each metric.

recovery and of RMSE.

6 Real data analysis

In this section, we apply SOFIA to a real-world economic dataset to identify the most relevant functional predictors to predict future GDP growth in Canada. Our goal is twofold: first, to assess

SOFIA’s capacity to select meaningful variables in a high-dimensional real dataset; second, to evaluate the predictive performance of SOFIA compared to classic forecasting methods and classic functional regression. The time-varying nature of economic and financial data makes FDA highly relevant for their analysis. One challenge in these research areas is the high frequency of the data, which can lead to overfitting, noise, and computational complexity. FDA offers robust methods to handle and analyze high-frequency data by smoothing and leveraging their continuous nature (Zhang et al., 2023). Another challenge is the heterogeneity of the data time frequencies: some variables are reported monthly, while others are reported quarterly or annually (Kapetanios et al., 2016). In FDA, different measurement frequencies are easily managed because all variables are transformed into curves on a continuous domain and can then be evaluated on the same grid. For recent applications of FSA in economy and finance see, e.g., Reimherr et al. (2018); Severino et al. (2022); Cremona et al. (2023)

The prediction of GDP growth is crucial for macroeconomic analysis, as it helps policymakers, financial institutions, and businesses to make decisions. We are interested in cases where multiple macroeconomic predictors are observed and we want to determine the relevant variables to predict GDP growth. We use a dataset from Fortin-Gagnon et al. (2022), which provides a comprehensive macroeconomic database on Canadian economic indicators. We consider a balanced version of the data that overcomes the issues related to stationarity, missing data, and discontinuities. We use monthly data from January 1981 to December 2019, resulting in 468 monthly observations. This time frame excludes the unpredictable outbreak of the COVID-19 pandemic. The dataset includes many international, national, and provincial economic variables. To ensure meaningful and interpretable results, we restrict our analysis to national-level indicators and select 20 variables that are commonly used in GDP prediction studies. These variables represent various financial sectors and include predictors such as total GDP growth (`GDP_new`), industrial production GDP growth (`IP_new`), retail trade GDP (`RT_new`) growth, public administration GDP growth (`PA_new`), oil production (`OIL_CAN_new`), employment rate (`EMP_CAN`), unemployment rate (`UNEMP_CAN`), new housing price index (`NHOUSE_P_CAN`), housing starts units (`Hstart_CAN_new`), total building permits (`build.Total_CAN_new`), M3 money supply (`M3`), household credit (`CRED_HOUS`), business credit (`CRED_BUS`), bank rate (`BANK_RATE_L`), three-month Treasury bill rate (`TBILL_3M`), total Canada’s official international reserves (`RES_TOT`), total imports (`Imp_BP_new`), total exports (`Exp_BP_new`), exchange rate between the US and the Canadian dollar (`USDCAD_new`), and the inflation rate measured by the Consumer Price Index (`CPI_ALL_CAN`). For complete definitions of the variables, see Fortin-Gagnon et al. (2022).

We construct functional predictors using monthly data by considering 12 consecutive values as a curve. We do not apply additional smoothing, so that the functional representation preserves the original structure of the data. Indeed, since data have been transformed in the original paper to reach stationarity, smoothing would artificially flatten the curves filtering out important information. To generate enough observations, we employ a rolling window method with a one-month shift. Precisely, each functional observation corresponds to a sequence of 12 consecutive months: the first observation consists of a curve obtained by the data from months 1 to 12, the second from months 2 to 13, and so on. Following this procedure, we obtain a dataset that contains 456 observations and 20 predictors. For the scalar response, we consider the GDP growth of the month immediately following the 12-month predictors. GDP growth is measured as the change in GDP from one month to the next, using the difference of logarithmic values. This transformed variable is called `GDP_new` in the dataset of Fortin-Gagnon et al. (2022).

Since we want to compare the predictive performance of SOFIA with other methods, we designate the final 36 months of the dataset as the test set for prediction comparison, while the

remaining 420 observations are used for fitting the models. We run SOFIA with an exponential kernel and parameter 2, which is well-suited for handling rough data (the functional predictors are not smoothed) and exhibits good robustness to noise. For the selection of λ , we use a grid of 100 candidate values with a ratio of 0.1, and a rolling-window cross-validation. Specifically, the first 315 observations (75% of the data) are used as the initial training set, while the next 21 observations (5% of the data) are used as the test set. In each subsequent fold, we shift both the training and test sets forward by 21 observations (5% of the data). This procedure results in a 5-fold rolling-window cross-validation framework.

SOFIA selects three functional predictors, namely the total GDP growth (`GDP_new`), employment rate (`EMP_CAN`), and unemployment rate (`UNEMP_CAN`). Figure 4 presents the estimated $\hat{\beta}$ coefficients corresponding to the selected predictors. The estimated coefficient functions reveal that the GDP growth and employment rate have a positive relation with the GDP growth of the next month, and their effects grow stronger over time until the 10th month. This suggests that, in the prediction of GDP growth, the GDP growth rate observed three months before has the highest predictive power relative to the other months. In contrast, the unemployment rate shows a negative effect, indicating that higher unemployment is associated with lower GDP growth. Similarly to the other two selected variables, the values of the three months preceding the forecast month are the most influential for this predictor. Interestingly, at the beginning of the period, all three predictors show a pattern opposite to what is observed later. This may suggest a form of mean reversion, where early movements are gradually offset or reversed as the economy adjusts over time.

We compare the performance of SOFIA with three classic time series models as benchmarks: the AutoRegressive Integrated Moving Average (ARIMA), the AutoRegressive Integrated Moving Average with Exogenous Regressors (ARIMAX; Gu et al., 2022), and the naïve model that forecasts the next GDP growth as the last observed value of GDP growth. In addition, we consider a simple scalar-on-function regression model (without penalization) that uses only `GDP_new` as functional predictor. We estimate ARIMA and ARIMAX using the function `auto.arima()` from the R package **forecast** (with default parameters), which automatically selects the optimal parameters based on the corrected Akaike Information Criterion. Then, we give the fitted models as input to the `Arima()` function to forecast GDP growth for the following month on the test set without reestimating the model. In ARIMAX, we include as exogenous variables all the predictors employed by SOFIA at time $t - 1$, ensuring a fair comparison in terms of the variables considered. As for the simple scalar-on-function model, we implement it using a non-penalized version of SOFIA (i.e., setting $\lambda = 0$). To compare the predictive performance of the methods, we calculate the prediction error as the root mean squared error (RMSE) and the mean absolute value (MAE) over the 36 months in the test set.

Table 3 shows the test RMSE and MAE for the size compared methods. For readability, all RMSE and MAE values in the table are multiplied by 100. The ARIMA model selected by `auto.arima()` is an ARIMA(4,0,5) with a nonzero mean, while the selected ARIMAX model has ARIMA(3,0,0) errors. We observe that SOFIA achieves the lowest prediction error among the considered methods, slightly outperforming ARIMA in both RMSE and MAE. Although the ARIMAX model shows a marginal improvement in MAE compared to ARIMA, its RMSE is higher, suggesting that the inclusion of all exogenous predictors does not consistently enhance forecast accuracy. The Simple scalar-on-function regression model performs moderately well but is clearly outperformed by SOFIA, as expected. This highlights the benefit of selecting informative predictors through the SOFIA procedure rather than relying on a single functional covariate.

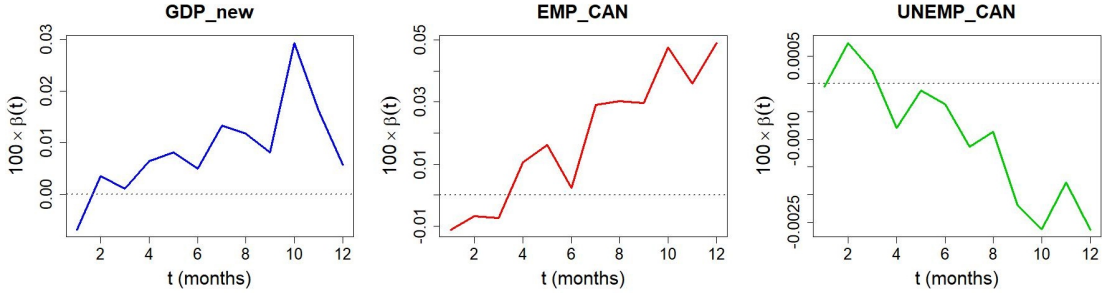


Figure 4: Estimated coefficients ($\hat{\beta}$) for the three selected predictors for GDP growth.

Model	ARIMA	ARIMAX	Naïve	Simple SoF	SOFIA
RMSE	0.2163	0.2361	0.2625	0.2234	0.2125
MAE	0.1781	0.1742	0.1939	0.1830	0.1651

Table 3: Test RMSE and MAE ($\times 100$) for the different methods.

7 Conclusions and future work

In this paper, we introduced a novel method, named SOFIA, for variable selection in scalar-on-function regression models, which enables the estimation of functional coefficients with a desired level of smoothness (or, more in general, regularity). To achieve this goal, we require the coefficients to lie in an RKHS-type space that determines the smoothness level, while allowing the predictors to reside in a general Hilbert space. We showed that SOFIA satisfies the functional oracle property, even in scenarios where the number of predictors is much larger than the sample size. In an extensive simulation study, we demonstrated the advantages of our method in variable selection and prediction accuracy with respect to other existing methods.

Our approach adopts a sieve truncation on the eigenbasis of the operator K and solves the penalized least squares with functional subgradients. This strategy yields a sequence of finite-dimensional problems on nested subspaces $\mathbb{K}^{(m)}$ and leads to nonparametric convergence rates that explicitly depend on the sieve level and the complexity of the design. However, selecting the optimal value for the dimension m remains an open problem. Moreover, the representer theorem offers an alternative that enables the study of analytical properties without truncation. This approach is more closely aligned with nonparametric methods and is left for future work.

The literature in the area of functional variable selection is limited, and there is a great space for future research. For instance, we assume that the functional predictors are fully observed and are not contaminated by noise, whereas, in practice, the variables are noisy and observed on a finite grid. Considering the effect of noise and grid size remains an open issue. More broadly, SOFIA is a linear regression method with a lasso penalty. As time-varying data acquisition advances, the need for more complex statistical tools (nonlinear methods or more complex penalties) becomes increasingly more important. This evolution introduces numerous theoretical and computational challenges that push the research agenda in FDA and, in particular, in functional regression models.

References

- Aneiros, G., S. Novo, and P. Vieu (2022). Variable selection in functional regression models: A review. *Journal of Multivariate Analysis* 188, 104871.
- Barber, R. F., M. Reimherr, and T. Schill (2017). The function-on-scalar LASSO with applications to longitudinal GWAS. *Electronic Journal of Statistics* 11, 1351–1389.
- Bauschke, H. H., P. L. Combettes, et al. (2011). *Convex Analysis and Monotone Operator Theory in Hilbert Spaces*, Volume 408. Springer.
- Bellec, P. and A. Tsybakov (2017). Bounds on the prediction error of penalized least squares estimators with convex penalty. In *Modern Problems of Stochastic Analysis and Statistics: Selected Contributions In Honor of Valentin Konakov*, pp. 315–333. Springer.
- Berlinet, A. and C. Thomas-Agnan (2011). *Reproducing Kernel Hilbert Spaces in Probability and Statistics*. Springer Science & Business Media.
- Berrrendero, J. R., B. Bueno-Larraz, and A. Cuevas (2019). An RKHS model for variable selection in functional linear regression. *Journal of Multivariate Analysis* 170, 25–45.
- Bickel, P. J., Y. Ritov, and A. B. Tsybakov (2009). Simultaneous analysis of Lasso and Dantzig selector. *The Annals of Statistics* 38(4), 1705—1732.
- Boschi, T., L. Testa, F. Chiaromonte, and M. Reimherr (2025). FASTen: an efficient adaptive method for feature selection and estimation in high-dimensional functional regressions. *Journal of Computational and Graphical Statistics* 34(2), 567–579.
- Boucheron, S., G. Lugosi, and O. Bousquet (2013). Concentration inequalities. In *Summer School on Machine Learning*, pp. 208–240. Springer.
- Bühlmann, P. and S. Van De Geer (2011). *Statistics for High-dimensional Data: Methods, Theory, and Applications*. Springer Science & Business Media.
- Campos-Sánchez, R., M. A. Cremona, A. Pini, F. Chiaromonte, and K. D. Makova (2016, 06). Integration and fixation preferences of human and mouse endogenous retroviruses uncovered with functional data analysis. *PLoS Computational Biology* 12(6), 1–41.
- Cardot, H., C. Crambes, and P. Sarda (2007). Ozone pollution forecasting using conditional mean and conditional quantiles with functional covariates. *Statistical methods for biostatistics and related fields*, 221–243.
- Chen, D., M. A. Cremona, Z. Qi, R. D. Mitra, F. Chiaromonte, and K. D. Makova (2020). Human L1 transposition dynamics unraveled with functional data analysis. *Molecular biology and evolution* 37(12), 3576–3600.
- Cremona, M. A., L. Doroshenko, and F. Severino (2023). Functional motif discovery in stock market prices. *SSRN* (4642040).
- Fan, J. and R. Li (2001). Variable selection via nonconcave penalized likelihood and its oracle properties. *Journal of the American Statistical Association* 96(456), 1348–1360.
- Fan, Y., G. M. James, and P. Radchenko (2015). Functional additive regression. *The Annals of Statistics* 43(5), 2296–2325.
- Fan, Z. and M. Reimherr (2017). High-dimensional adaptive function-on-scalar regression. *Econometrics and Statistics* 1, 167–183.

- Fortin-Gagnon, O., M. Leroux, D. Stevanovic, and S. Surprenant (2022). A large Canadian database for macroeconomic analysis. *Canadian Journal of Economics* 55(4), 1799–1833.
- Genton, M. G. (2001). Classes of kernels for machine learning: a statistics perspective. *Journal of Machine Learning Research* 2(Dec), 299–312.
- Gertheiss, J., A. Maity, and A.-M. Staicu (2013). Variable selection in generalized functional linear models. *Stat* 2(1), 86–101.
- Gu, Y., Z. Shao, X. Huang, and B. Cai (2022). GDP forecasting model for china’s provinces using nighttime light remote sensing data. *Remote Sensing* 14(15), 3671.
- Hanke, M., L. Dijkstra, R. Foraita, and V. Didelez (2024). Variable selection in linear regression models: Choosing the best subset is not always the best choice. *Biometrical Journal* 66(1), 2200209.
- Hsing, T. and R. Eubank (2015). *Theoretical Foundations of Functional Data Analysis, with an Introduction to Linear Operators*, Volume 997. John Wiley & Sons.
- Huang, J., S. Ma, and C.-H. Zhang (2008). Adaptive lasso for sparse high-dimensional regression models. *Statistica Sinica* 18, 1603–1618.
- Huang, L., J. Zhao, H. Wang, and S. Wang (2016). Robust shrinkage estimation and selection for functional multiple linear model through LAD loss. *Computational Statistics & Data Analysis* 103, 384–400.
- Insolia, L., A. Kenney, F. Chiaromonte, and G. Felici (2022). Simultaneous feature selection and outlier detection with optimality guarantees. *Biometrics* 78(4), 1592–1603.
- Kadri, H., E. Duflos, P. Preux, S. Canu, and M. Davy (2010). Nonlinear functional regression: a functional RKHS approach. In *Proceedings of the Thirteenth International Conference on Artificial Intelligence and Statistics*, pp. 374–380. JMLR Workshop and Conference Proceedings.
- Kapetanios, G., M. Marcellino, and F. Papailias (2016). Forecasting inflation and GDP growth using heuristic optimisation of information criteria and variable reduction methods. *Computational Statistics & Data Analysis* 100, 369–382.
- Kokoszka, P. and M. Reimherr (2017). *Introduction to Functional Data Analysis*. Chapman and Hall/CRC.
- Lian, H. (2013). Shrinkage estimation and selection for multiple functional regression. *Statistica Sinica* 23, 51–74.
- Lounici, K., M. Pontil, S. Van De Geer, and A. B. Tsybakov (2011). Oracle inequalities and optimal inference under group sparsity. *The Annals of Statistics* 39(4), 2164–2204.
- Matsui, H. and S. Konishi (2011). Variable selection for functional regression models via the L_1 regularization. *Computational Statistics & Data Analysis* 55(12), 3304–3310.
- Mirshani, A. and M. Reimherr (2021). Adaptive function-on-scalar regression with a smoothing elastic net. *Journal of Multivariate Analysis* 185, 104765.
- Murphy, G. J. (1990). *C*-Algebras and Operator Theory*. San Diego: Academic Press.
- Parodi, A. and M. Reimherr (2018). Simultaneous variable selection and smoothing for high-dimensional function-on-scalar regression. *Electronic Journal of Statistics* 12(2), 4602–4639.
- Ramsay, J. O. and B. W. Silverman (2005). *Functional Data Analysis* (2 ed.). Springer.
- Reimherr, M., B. Sriperumbudur, and B. Taoufik (2018). Optimal prediction for additive function-on-function regression. *Electronic Journal of Statistics* 12, 4571—4601.

- Roche, A. (2023). Lasso in infinite dimension: application to variable selection in functional multivariate linear regression. *Electronic Journal of Statistics* 17(2), 3357–3405.
- Severino, F., M. A. Cremona, and É. Dadié (2022). COVID-19 effects on the Canadian term structure of interest rates. *Review of Economic Analysis* 14(4), 471–502.
- Shin, H. and S. Lee (2016). An RKHS approach to robust functional linear regression. *Statistica Sinica* 26(1), 255–272.
- Tibshirani, R. (1996). Regression shrinkage and selection via the lasso. *Journal of the Royal Statistical Society Series B: Statistical Methodology* 58(1), 267–288.
- Ullah, S. and C. F. Finch (2013). Applications of functional data analysis: A systematic review. *BMC Medical Research Methodology* 13, 1–12.
- Wang, D., Z. Zhao, Y. Yu, and R. Willett (2022). Functional linear regression with mixed predictors. *Journal of Machine Learning Research* 23(266), 1–94.
- Wang, J.-L., J.-M. Chiou, and H.-G. Müller (2016). Functional data analysis. *Annual Review of Statistics and its Application* 3(1), 257–295.
- Widom, H. (1964). Asymptotic behavior of the eigenvalues of certain integral equations. II. *Archive for Rational Mechanics and Analysis* 17(3), 215–229.
- Yuan, M. and T. T. Cai (2010). A reproducing kernel Hilbert space approach to functional linear regression. *The Annals of Statistics* 38(6), 3412–3444.
- Yuan, M. and Y. Lin (2006). Model selection and estimation in regression with grouped variables. *Journal of the Royal Statistical Society Series B: Statistical Methodology* 68(1), 49–67.
- Zhang, X., Y. Huang, K. Xu, and L. Xing (2023). Novel modeling strategies for high-frequency stock trading data. *Financial Innovation* 9(1), 39.
- Zhao, P. and B. Yu (2006). On model selection consistency of lasso. *The Journal of Machine Learning Research* 7, 2541–2563.
- Zou, H. (2006). The adaptive lasso and its oracle properties. *Journal of the American Statistical Association* 101(476), 1418–1429.

Selection of functional predictors and smooth coefficient estimation for scalar-on-function regression models

Supplementary material

Hedayat Fathi

Department of Operations and Decision Systems, Université Laval, Québec, Canada
hedayat.fathi.1@ulaval.ca

Marzia A. Cremona

Chair in Statistical Learning and Department of Operations and Decision Systems, Université Laval, Québec, Canada
marzia.cremona@fsa.ulaval.ca

Federico Severino

Department of Finance, Insurance and Real Estate, Université Laval, Québec, Canada
federico.severino@fsa.ulaval.ca

This supplementary material is organized as follows. Section S1 provides additional theoretical results related to the mathematical framework presented in Section 2, as well as the proofs of the theoretical results presented in Section 3 and of the functional subgradient formula presented in Section 4; Section S2 presents additional simulation results.

S1 Additional theoretical results and proofs

S1.1 Characterization of the Hilbert space \mathbb{K}

In this subsection, we explicitly characterize the Hilbert space \mathbb{K} defined by (4). Let $R(K)$ denote the range of the operator $K : \mathbb{H} \rightarrow \mathbb{H}$. For any $h \in R(K)$, the range norm of h is

$$\|h\|_{R(K)} = \inf \{\|g\|_{\mathbb{H}} : K(g) = h\}.$$

With this norm, $R(K)$ is a Hilbert space, although $R(K)$ is never closed in \mathbb{H} if K has infinite rank. Since 0 is assumed to not be an eigenvalue of K , K is injective, so we can define $\|h\|_{R(K)}$ using the preimage of h . This formulation ensures that the pair $(R(K), \|\cdot\|_{R(K)})$ allows the following operator to be a surjective isometry: $K : (\mathbb{H}, \|\cdot\|_{\mathbb{H}}) \rightarrow (R(K), \|\cdot\|_{R(K)})$. For further details, see Sarason (2007) and Paulsen and Raghupathi (2016).

Proposition S1 elucidates the structure of the coefficient space \mathbb{K} , showing that it coincides with the range of $K^{1/2}$. This characterization enables the computation of \mathbb{K} -norms based on \mathbb{H} -norms. It also demonstrates that the assumption that the coefficients belong to the subspace \mathbb{K} is not

overly restrictive. Indeed, since all the eigenvalues of K are assumed to be nonzero, the spectral mapping theorem implies that $K^{1/2}$ also has nonzero eigenvalues. Consequently, its null space is zero and its range is dense in \mathbb{H} with respect to the topology induced by the norm of \mathbb{H} .

Proposition S1. *If K has the spectral decomposition (4), then the Hilbert space \mathbb{K} coincides with $(R(K^{1/2}), \|\cdot\|_{R(K^{1/2})})$ as a Hilbert space.*

Proof. First, we show that $R(K^{1/2}) = \mathbb{K}$, and then discuss the equality of norms. Let $h \in R(K^{1/2})$. Then there exists $g \in \mathbb{H}$ such that $h = K^{1/2}(g)$. Using the self-adjointness of K and Parseval's identity, we have the following.

$$\sum_{l=1}^{+\infty} \frac{|\langle h, v_l \rangle_{\mathbb{H}}|^2}{\theta_l} = \sum_{l=1}^{+\infty} \frac{|\langle K^{1/2}(g), v_l \rangle_{\mathbb{H}}|^2}{\theta_l} = \sum_{l=1}^{+\infty} |\langle g, v_l \rangle_{\mathbb{H}}|^2 = \|g\|_{\mathbb{H}}^2.$$

This proves that $h \in \mathbb{K}$. To prove the reverse, let $h \in \mathbb{K}$ and define $g = \sum_{l=1}^{\infty} (\langle h, v_l \rangle / \sqrt{\theta_l}) v_l$. Observe that g is well defined by the definition of \mathbb{K} . Moreover, by another use of the self-adjointness of K and Parseval's identity, we have

$$K^{1/2}(g) = K^{1/2} \left(\sum_{l=1}^{+\infty} \frac{\langle h, v_l \rangle_{\mathbb{H}} v_l}{\sqrt{\theta_l}} \right) = \sum_{l=1}^{+\infty} \langle h, v_l \rangle_{\mathbb{H}} v_l = h.$$

Therefore, $h \in R(K^{1/2})$.

The following argument shows that the two norms are equal. Let $h \in \mathbb{K} = R(K^{1/2})$. Then, there exists $g \in \mathbb{H}$ such that $K^{1/2}(g) = h$. Now, we have

$$\|h\|_{R(K^{1/2})}^2 = \|g\|_{\mathbb{H}}^2 = \sum_{l=1}^{+\infty} \langle g, v_l \rangle_{\mathbb{H}}^2 = \sum_{l=1}^{+\infty} \theta_l \frac{\langle g, v_l \rangle_{\mathbb{H}}^2}{\theta_l} = \sum_{l=1}^{+\infty} \frac{\langle h, v_l \rangle_{\mathbb{H}}^2}{\theta_l} = \|h\|_{\mathbb{K}}^2.$$

□

S1.2 Approximation error

Proposition S2. *Let X_j and β_j^* satisfy Assumption 2 for all $j \in \mathcal{A}$. Then, as the dimension m increases, the approximation error in eq. (5) tends to zero uniformly.*

Proof. The expansions of the predictors and the coefficients are

$$X_{ij} = \sum_{l=1}^{+\infty} \langle X_{ij}, v_l \rangle_{\mathbb{H}} v_l, \quad \beta_j^* = \sum_{l=1}^{+\infty} \langle \beta_j^*, v_l \rangle_{\mathbb{H}} v_l,$$

and the inner product can then be expressed as

$$\langle \beta_j^*, X_{ij} \rangle_{\mathbb{H}} = \sum_{l=1}^{+\infty} \langle \beta_j^*, v_l \rangle_{\mathbb{H}} \langle X_{ij}, v_l \rangle_{\mathbb{H}}.$$

By restricting to a finite-dimensional subspace $\mathbb{H}^{(m)}$, the latter becomes

$$\langle \beta_j^*, X_{ij} \rangle_{\mathbb{H}} = \left\langle \beta_j^{*(m)}, X_{ij}^{(m)} \right\rangle_{\mathbb{H}} + e_{ij}, \quad e_{ij} = \sum_{l=m+1}^{+\infty} \langle \beta_j^*, v_l \rangle_{\mathbb{H}} \langle X_{ij}, v_l \rangle_{\mathbb{H}},$$

where e_{ij} is the approximation error. Using the Cauchy-Schwarz inequality, we get

$$e_{ij}^2 = \left(\sum_{l=m+1}^{+\infty} \langle \beta_j^*, v_l \rangle_{\mathbb{H}} \langle X_{ij}, v_l \rangle_{\mathbb{H}} \right)^2 \leq \sum_{l=m+1}^{+\infty} \theta_l^{-1} \langle \beta_j^*, v_l \rangle_{\mathbb{H}}^2 \sum_{l=m+1}^{+\infty} \theta_l \langle X_{ij}, v_l \rangle_{\mathbb{H}}^2.$$

By Assumption 2, we have the bounds

$$\sum_{l=m+1}^{+\infty} \theta_l^{-1} \langle \beta_j^*, v_l \rangle_{\mathbb{H}}^2 \leq \|\beta_j^*\|_{\mathbb{K}}^2 \leq b_1^2 \quad \text{and} \quad \sum_{l=m+1}^{+\infty} \theta_l \langle X_{ij}, v_l \rangle_{\mathbb{H}}^2 \leq b_2 \sum_{l=m+1}^{+\infty} l^{-\gamma}$$

with $\gamma > 1$. By applying the integral test, there exists a constant C such that $\sum_{l=m+1}^{+\infty} l^{-\gamma} \leq C m^{-(\gamma-1)}$. As a result, the squared error is bounded as $e_{ij}^2 \leq b_1^2 b_2 C m^{-(\gamma-1)}$.

Taking square roots gives $e_{ij} \leq b_1 (b_2 C)^{1/2} m^{-(\gamma-1)/2}$. Summing over the active set \mathcal{A} and using the triangle inequality,

$$\sum_{j \in \mathcal{A}} e_{ij} \leq b_1 (b_2 C)^{1/2} p_0 m^{-(\gamma-1)/2}.$$

By Assumption 2, $p_0 = o(m^{(\gamma-1)/2})$, therefore $\sum_{j \in \mathcal{A}} e_{ij} = o(1)$ when $m \rightarrow +\infty$. For $j \notin \mathcal{A}$ we have $\beta_j^* = 0$, so $e_{ij} = 0$ and the approximation error vanishes. This completes the proof. \square

S1.3 RE condition

In Proposition S3 we show that, if φ_m and $\|\hat{\Gamma}_{\mathbf{X}_2}\|_{op}$ tend to zero sufficiently fast, the RE condition is satisfied under Assumption 4.

Proposition S3. *Let points 1 and 3 of Assumption 4 hold. Assume that*

$$\tau_m^{-1} > 9p_0 \sigma_{max} \left(\hat{\Gamma}_{\mathbf{X}_2}^{(m)} \right) + 6\sqrt{p_0} \tau \varphi_m.$$

Then, there exists $\alpha_m > 0$ such that, for any $\boldsymbol{\delta} \in \mathbb{K}^{(m)p}$ with $\|\boldsymbol{\delta}_{\mathcal{A}^{(m)C}}\|_{\ell_1/\mathbb{K}} \leq 3\|\boldsymbol{\delta}_{\mathcal{A}^{(m)}}\|_{\ell_1/\mathbb{K}}$, we have $\|\hat{\Gamma}_{\mathbf{X}\mathbf{X}}^{(m)1/2} \boldsymbol{\delta}\|_{\mathbb{K}} \geq \alpha_m \|\boldsymbol{\delta}\|_{\mathbb{K}}$.

Proof. Let $\boldsymbol{\delta} \in \mathbb{K}^{(m)}$ satisfy $\|\boldsymbol{\delta}_{\mathcal{A}^{(m)C}}\|_{\ell_1/\mathbb{K}} \leq 3\|\boldsymbol{\delta}_{\mathcal{A}^{(m)}}\|_{\ell_1/\mathbb{K}}$. By the block structure of $\hat{\Gamma}_{\mathbf{X}\mathbf{X}}^{(m)}$ we have

$$\begin{aligned} \left\| \hat{\Gamma}_{\mathbf{X}\mathbf{X}}^{(m)1/2}(\boldsymbol{\delta}) \right\|_{\mathbb{K}}^2 &= \left\langle \hat{\Gamma}_{\mathbf{X}\mathbf{X}}^{(m)}(\boldsymbol{\delta}), \boldsymbol{\delta} \right\rangle_{\mathbb{K}} = \left\langle \hat{\Gamma}_{\mathbf{X}_1}^{(m)}(\boldsymbol{\delta}_{\mathcal{A}^{(m)}}), \boldsymbol{\delta}_{\mathcal{A}^{(m)}} \right\rangle_{\mathbb{K}} \\ &\quad + \left\langle \hat{\Gamma}_{\mathbf{X}_2}^{(m)}(\boldsymbol{\delta}_{\mathcal{A}^{(m)C}}), \boldsymbol{\delta}_{\mathcal{A}^{(m)C}} \right\rangle_{\mathbb{K}} + 2 \left\langle \hat{\Gamma}_{\mathbf{X}_1\mathbf{X}_2}^{(m)}(\boldsymbol{\delta}_{\mathcal{A}^{(m)C}}), \boldsymbol{\delta}_{\mathcal{A}^{(m)C}} \right\rangle_{\mathbb{K}}. \end{aligned}$$

We bound all the terms on the left-hand side. For the first one, we use point 1 of Assumption 4:

$$\left\langle \hat{\Gamma}_{\mathbf{X}_1}^{(m)}(\boldsymbol{\delta}_{\mathcal{A}^{(m)}}), \boldsymbol{\delta}_{\mathcal{A}^{(m)}} \right\rangle_{\mathbb{K}} \geq \tau_m^{-1} \|\boldsymbol{\delta}_{\mathcal{A}^{(m)}}\|^2.$$

For the second one, we can write

$$\begin{aligned} \left\langle \hat{\Gamma}_{\mathbf{X}_2}^{(m)}(\boldsymbol{\delta}_{\mathcal{A}^{(m)C}}), \boldsymbol{\delta}_{\mathcal{A}^{(m)C}} \right\rangle_{\mathbb{K}} &\leq \sigma_{max}(\hat{\Gamma}_{\mathbf{X}_2}^{(m)}) \|\boldsymbol{\delta}_{\mathcal{A}^{(m)C}}\|^2 \leq \sigma_{max}(\hat{\Gamma}_{\mathbf{X}_2}^{(m)}) \|\boldsymbol{\delta}_{\mathcal{A}^{(m)C}}\|_{\ell_1/\mathbb{K}}^2 \\ &\leq 9 \sigma_{max}(\hat{\Gamma}_{\mathbf{X}_2}^{(m)}) \|\boldsymbol{\delta}_{\mathcal{A}^{(m)}}\|_{\ell_1/\mathbb{K}}^2 \leq 9 p_0 \sigma_{max}(\hat{\Gamma}_{\mathbf{X}_2}^{(m)}) \|\boldsymbol{\delta}_{\mathcal{A}^{(m)}}\|^2. \end{aligned}$$

For the third one, we have

$$\begin{aligned}
2 \left\langle \hat{\Gamma}_{\mathbf{X}_1 \mathbf{X}_2}^{(m)}(\boldsymbol{\delta}_{\mathcal{A}^{(m)C}}), \boldsymbol{\delta}_{\mathcal{A}} \right\rangle_{\mathbb{K}} &= 2 \left\langle \hat{\Gamma}_{\mathbf{X}_1}^{(m)} \hat{\Gamma}_{\mathbf{X}_1}^{(m)-1} \hat{\Gamma}_{\mathbf{X}_1 \mathbf{X}_2}^{(m)}(\boldsymbol{\delta}_{\mathcal{A}^{(m)C}}), \boldsymbol{\delta}_{\mathcal{A}^{(m)}} \right\rangle_{\mathbb{K}} \\
&\leq 2\tau \left\| \hat{\Gamma}_{\mathbf{X}_1}^{(m)-1} \hat{\Gamma}_{\mathbf{X}_1 \mathbf{X}_2}^{(m)} \right\|_{op} \|\boldsymbol{\delta}_{\mathcal{A}^{(m)}}\|_{\mathbb{K}} \|\boldsymbol{\delta}_{\mathcal{A}^{(m)C}}\|_{\ell_1/\mathbb{K}} \\
&\leq 6\tau\varphi_m \|\boldsymbol{\delta}_{\mathcal{A}^{(m)}}\|_{\ell_1/\mathbb{K}}^2 \leq 6\sqrt{p_0}\tau\varphi_m \|\boldsymbol{\delta}_{\mathcal{A}^{(m)}}\|_{\mathbb{K}}^2.
\end{aligned}$$

Now, by summing together all the bounds and using the triangle inequality,

$$\begin{aligned}
\left\| \hat{\Gamma}_{\mathbf{X}\mathbf{X}}^{(m)1/2}(\boldsymbol{\delta}) \right\|_{\mathbb{K}}^2 &\geq \left\langle \hat{\Gamma}_{\mathbf{X}_1}^{(m)}(\boldsymbol{\delta}_{\mathcal{A}^{(m)}}), \boldsymbol{\delta}_{\mathcal{A}^{(m)}} \right\rangle_{\mathbb{K}} - \left\langle \hat{\Gamma}_{\mathbf{X}_2}^{(m)}(\boldsymbol{\delta}_{\mathcal{A}^{(m)C}}), \boldsymbol{\delta}_{\mathcal{A}^{(m)C}} \right\rangle_{\mathbb{K}} - 2 \left\langle \hat{\Gamma}_{\mathbf{X}_2 \mathbf{X}_1}^{(m)}(\boldsymbol{\delta}_{\mathcal{A}^{(m)}}), \boldsymbol{\delta}_{\mathcal{A}^{(m)C}} \right\rangle_{\mathbb{K}} \\
&\geq \left(\tau_m^{-1} - 9p_0\sigma_{\max}(\hat{\Gamma}_{\mathbf{X}_2}^{(m)}) - 6\sqrt{p_0}\tau\varphi_m \right) \|\boldsymbol{\delta}_{\mathcal{A}^{(m)}}\|_{\mathbb{K}}^2.
\end{aligned}$$

Finally, we convert $\|\boldsymbol{\delta}_{\mathcal{A}^{(m)}}\|_{\mathbb{K}}$ to $\|\boldsymbol{\delta}\|_{\mathbb{K}}$

$$\|\boldsymbol{\delta}\|_{\mathbb{K}} \leq \|\boldsymbol{\delta}_{\mathcal{A}^{(m)}}\|_{\mathbb{K}} + \|\boldsymbol{\delta}_{\mathcal{A}^{(m)C}}\|_{\mathbb{K}} \leq \|\boldsymbol{\delta}_{\mathcal{A}^{(m)}}\|_{\mathbb{K}} + 3\|\boldsymbol{\delta}_{\mathcal{A}^{(m)}}\|_{\ell_1/\mathbb{K}} \leq (1+3\sqrt{p_0})\|\boldsymbol{\delta}_{\mathcal{A}^{(m)}}\|_{\mathbb{K}} \leq 4\sqrt{p_0}\|\boldsymbol{\delta}_{\mathcal{A}^{(m)}}\|_{\mathbb{K}}.$$

Therefore,

$$\left\| \hat{\Gamma}_{\mathbf{X}\mathbf{X}}^{(m)1/2} \boldsymbol{\delta} \right\|_{\mathbb{K}} \geq \frac{1}{4\sqrt{p_0}} \sqrt{\tau_m^{-1} - 6\sqrt{p_0}\tau\varphi_m - 9p_0\sigma_{\max}(\hat{\Gamma}_{\mathbf{X}_2}^{(m)})} \|\boldsymbol{\delta}\|_{\mathbb{K}}.$$

We obtain the desired result by defining

$$\alpha_m = \frac{1}{4\sqrt{p_0}} \sqrt{\tau_m^{-1} - 9p_0\sigma_{\max}(\hat{\Gamma}_{\mathbf{X}_2}^{(m)}) - 6\sqrt{p_0}\tau\varphi_m}.$$

□

In particular, if $\tau_m^{-1} \sim m^{-2\kappa}$, $\varphi_m \ll m^{-\kappa}$ and $\sigma_{\max}(\hat{\Gamma}_{\mathbf{X}_2}^{(m)}) \ll m^{-2\kappa}$, then the RE condition is satisfied and $\alpha_m \asymp m^{-\kappa}/\sqrt{p_0}$.

S1.4 Proof of Lemma 1

Proof. Fix $j \in \{1, \dots, p\}$. By the Riesz representation theorem, we can represent the norm of Z as

$$\|Z_j\|_{\mathbb{H}} = \sup_{\|u\|_{\mathbb{H}}=1} \langle Z_j, u \rangle_{\mathbb{H}} = \sup_{\|u\|_{\mathbb{H}}=1} \frac{1}{n} \sum_{i=1}^n \varepsilon_i \langle X_{ij}, u \rangle_{\mathbb{H}}.$$

Fix any unit vector $u \in \mathbb{H}$, and define $a_i := \langle X_{ij}, u \rangle_{\mathbb{H}}$ for $i = 1, \dots, n$. Then,

$$\sum_{i=1}^n a_i^2 = \sum_{i=1}^n \langle X_{ij}, u \rangle_{\mathbb{H}}^2 \leq \sum_{i=1}^n \|X_{ij}\|_{\mathbb{H}}^2 = n,$$

by the Cauchy–Schwarz inequality. Let $b := \sum_{i=1}^n a_i^2$ and define the normalized coefficients $\tilde{a}_i := a_i/\sqrt{b}$ so that $\sum_{i=1}^n \tilde{a}_i^2 = 1$. We can now write

$$\langle Z_j, u \rangle_{\mathbb{H}} = \frac{1}{n} \sum_{i=1}^n a_i \varepsilon_i = \frac{\sqrt{b}}{n} \sum_{i=1}^n \tilde{a}_i \varepsilon_i.$$

Then, we apply Lemma 1 from the supplementary of Huang et al. (2008) to the normalized sum $\sum_{i=1}^n \tilde{a}_i \varepsilon_i$, which yields the existence of a constant M , such that for any $t > 0$,

$$P(\langle Z_j, u \rangle_{\mathbb{H}} > t) = P\left(\sum_{i=1}^n \tilde{a}_i \varepsilon_i > \frac{nt}{\sqrt{b}}\right) \leq \exp\left(-\frac{n^2 t^2}{bM}\right) \leq \exp\left(-\frac{nt^2}{M}\right),$$

where the final inequality follows from $b \leq n$. Since the bound holds uniformly over all $u \in \mathbb{H}$ with $\|u\|_{\mathbb{H}} = 1$ and there exists a u^* with unit norm such that $\|Z_j\|_{\mathbb{H}} = \langle Z_j, u^* \rangle_{\mathbb{H}}$, we obtain the claimed inequality. \square

S1.5 Proof of Theorem 1

Before proving Theorem 1, we state and prove two useful lemmas. Lemma S1 is a direct result of Lemma 1, which establishes a uniform concentration bound over a collection of Hilbert-valued processes $\{Z_j\}_{j=1}^p$.

Lemma S1. *Let $\mathbf{X} = (X_1, \dots, X_n)$ and $\boldsymbol{\varepsilon} = (\varepsilon_1, \dots, \varepsilon_n)$ be as in Assumption 1. For each $j = 1, \dots, p$, define $Z_j := n^{-1} \sum_{i=1}^n \varepsilon_i K(X_{ij})$. Consider $M > 0$ from Lemma 1 and, for any $\delta \in (0, 1)$, set $\lambda_0 := \sqrt{\theta_1 M \log(p/\delta)}/n$. Then,*

$$P\left(\max_{1 \leq j \leq p} \|Z_j\|_{\mathbb{K}} \leq \lambda_0\right) \geq 1 - \delta.$$

Proof. Fix any $j \in \{1, \dots, p\}$. Define $\tilde{Z}_j := n^{-1} \sum_{i=1}^n \varepsilon_i X_{ij} \in \mathbb{H}$. Then, $Z_j = K(\tilde{Z}_j) \in \mathbb{K}$ and, by Proposition S1, $\|Z_j\|_{\mathbb{K}} = \|K^{1/2}(\tilde{Z}_j)\|_{\mathbb{H}} \leq \sqrt{\theta_1} \|\tilde{Z}_j\|_{\mathbb{H}}$. Now, using Lemma 1, for all $t > 0$, we have

$$P(\|Z_j\|_{\mathbb{K}} > t) \leq P\left(\|\tilde{Z}_j\|_{\mathbb{H}} > t/\sqrt{\theta_1}\right) \leq \exp(-nt^2/\theta_1 M).$$

By the union bound over $j = 1, \dots, p$, we obtain

$$P\left(\max_{1 \leq j \leq p} \|Z_j\|_{\mathbb{K}} > t\right) \leq \sum_{j=1}^p P(\|Z_j\|_{\mathbb{K}} > t) \leq p \cdot \exp\left(-\frac{nt^2}{\theta_1 M}\right).$$

Finally, setting $t = \lambda_0$, we get $P(\max_{1 \leq j \leq p} \|Z_j\|_{\mathbb{K}} > \lambda_0) \leq \delta$. \square

Lemma S2 plays a central role in the proof of Theorem 1. It is the Hilbert-space analog of similar inequalities developed in the scalar setting by Barber et al. (2017).

Lemma S2. *Let Assumption 1 hold and $\tilde{\boldsymbol{\beta}}^{(m)}$ be a minimizer of the objective function (7) with weights equal to 1. If the tuning parameter λ satisfies*

$$\lambda \geq 2 \max_{1 \leq j \leq p} \left\| \frac{1}{n} \boldsymbol{\varepsilon}^\top K(X_j) \right\|_{\mathbb{K}},$$

then $\tilde{\boldsymbol{\beta}}^{(m)}$ satisfies

$$\left\| \hat{\Gamma}_{\mathbf{X}\mathbf{X}}^{(m)1/2} \left(\tilde{\boldsymbol{\beta}}^{(m)} - \boldsymbol{\beta}^{*(m)} \right) \right\|_{\mathbb{K}}^2 + \lambda \left\| \tilde{\boldsymbol{\beta}}_{\mathcal{A}^{(m)}e}^{(m)} \right\|_{\ell_1/\mathbb{K}} \leq 3\lambda \left\| \left(\tilde{\boldsymbol{\beta}}^{(m)} - \boldsymbol{\beta}^{*(m)} \right)_{\mathcal{A}^{(m)}} \right\|_{\ell_1/\mathbb{K}}.$$

Proof. For $i = 1, \dots, n$ and $j = 1, \dots, p$, we use the notation $K(\mathbf{X}^{(m)})_{ij} = K(X_{ij}^{(m)})$. The expression $\langle K(\mathbf{X}^{(m)}), \boldsymbol{\beta} \rangle_{\mathbb{K}}$ represents a vector in \mathbb{R}^n , whose i^{th} element is equal to $\sum_{j=1}^p \langle K(\mathbf{X}^{(m)})_{ij}, \beta_j \rangle_{\mathbb{K}}$. Since $\tilde{\boldsymbol{\beta}}^{(m)}$ is the minimizer, we have

$$\frac{1}{2n} \left| Y - \left\langle K(\mathbf{X}^{(m)}), \tilde{\boldsymbol{\beta}}^{(m)} \right\rangle_{\mathbb{K}} \right|^2 + \lambda \left\| \tilde{\boldsymbol{\beta}}^{(m)} \right\|_{\ell_1/\mathbb{K}} \leq \frac{1}{2n} \left| Y - \left\langle K(\mathbf{X}^{(m)}), \boldsymbol{\beta}^{*(m)} \right\rangle_{\mathbb{K}} \right|^2 + \lambda \left\| \boldsymbol{\beta}^{*(m)} \right\|_{\ell_1/\mathbb{K}},$$

where $|\cdot|$ is the Euclidean norm in \mathbb{R}^n . Additionally,

$$\begin{aligned} \frac{1}{2} \left| Y - \left\langle K(\mathbf{X}^{(m)}), \tilde{\boldsymbol{\beta}}^{(m)} \right\rangle_{\mathbb{K}} \right|^2 &= \frac{1}{2} \left| Y - \left\langle K(\mathbf{X}^{(m)}), \boldsymbol{\beta}^{*(m)} \right\rangle_{\mathbb{K}} \right|^2 \\ &\quad + \frac{1}{2} \left| \left\langle K(\mathbf{X}^{(m)}), \tilde{\boldsymbol{\beta}}^{(m)} - \boldsymbol{\beta}^{*(m)} \right\rangle_{\mathbb{K}} \right|^2 \\ &\quad - \left(Y - \left\langle K(\mathbf{X}^{(m)}), \boldsymbol{\beta}^{*(m)} \right\rangle_{\mathbb{K}} \right) \left(\left\langle K(\mathbf{X}^{(m)}), \tilde{\boldsymbol{\beta}}^{(m)} - \boldsymbol{\beta}^{*(m)} \right\rangle_{\mathbb{K}} \right)^{\top}. \end{aligned}$$

By the definition of norm, expanding the inner product and rearranging terms, we get

$$\begin{aligned} &\frac{1}{2} \left\| \hat{\Gamma}_{\mathbf{X}\mathbf{X}}^{(m)1/2} \left(\tilde{\boldsymbol{\beta}}^{(m)} - \boldsymbol{\beta}^{*(m)} \right) \right\|_{\mathbb{K}}^2 + \lambda \left\| \tilde{\boldsymbol{\beta}}^{(m)} \right\|_{\ell_1/\mathbb{K}} \\ &\leq \sum_{j=1}^p \left\langle \frac{1}{n} \boldsymbol{\varepsilon}^{\top} K(X_j^{(m)}), \tilde{\beta}_j^{(m)} - \beta_j^{*(m)} \right\rangle_{\mathbb{K}} + \lambda \left\| \boldsymbol{\beta}^{*(m)} \right\|_{\ell_1/\mathbb{K}} \\ &\leq \sum_{j=1}^p \left\| \frac{1}{n} \boldsymbol{\varepsilon}^{\top} K(X_j) \right\|_{\mathbb{K}} \left\| \tilde{\beta}_j^{(m)} - \beta_j^{*(m)} \right\|_{\mathbb{K}} + \lambda \left\| \boldsymbol{\beta}^{*(m)} \right\|_{\ell_1/\mathbb{K}} \\ &\leq \left(\max_{1 \leq j \leq p} \left\| \frac{1}{n} \boldsymbol{\varepsilon}^{\top} K(X_j) \right\|_{\mathbb{K}} \right) \left\| \tilde{\boldsymbol{\beta}}^{(m)} - \boldsymbol{\beta}^{*(m)} \right\|_{\ell_1/\mathbb{K}} + \lambda \left\| \boldsymbol{\beta}^{*(m)} \right\|_{\ell_1/\mathbb{K}}. \end{aligned}$$

Using this inequality, we conclude that

$$\left\| \hat{\Gamma}_{\mathbf{X}\mathbf{X}}^{(m)1/2} \left(\tilde{\boldsymbol{\beta}}^{(m)} - \boldsymbol{\beta}^{*(m)} \right) \right\|_{\mathbb{K}}^2 + 2\lambda \left\| \tilde{\boldsymbol{\beta}}^{(m)} \right\|_{\ell_1/\mathbb{K}} \leq \lambda \left\| \tilde{\boldsymbol{\beta}}^{(m)} - \boldsymbol{\beta}^{*(m)} \right\|_{\ell_1/\mathbb{K}} + 2\lambda \left\| \boldsymbol{\beta}^{*(m)} \right\|_{\ell_1/\mathbb{K}}. \quad (\text{S1})$$

Obviously, $\left\| \tilde{\boldsymbol{\beta}}^{(m)} \right\|_{\ell_1/\mathbb{K}} = \left\| \tilde{\boldsymbol{\beta}}_{\mathcal{A}^{(m)}}^{(m)} \right\|_{\ell_1/\mathbb{K}} + \left\| \tilde{\boldsymbol{\beta}}_{\mathcal{A}^{(m)C}}^{(m)} \right\|_{\ell_1/\mathbb{K}}$. Moreover, by the reverse triangle inequality,

$$\left\| \tilde{\boldsymbol{\beta}}_{\mathcal{A}^{(m)}}^{(m)} \right\|_{\ell_1/\mathbb{K}} \geq \left\| \boldsymbol{\beta}_{\mathcal{A}^{(m)}}^{*(m)} \right\|_{\ell_1/\mathbb{K}} - \left\| \tilde{\boldsymbol{\beta}}_{\mathcal{A}^{(m)}}^{(m)} - \boldsymbol{\beta}_{\mathcal{A}^{(m)}}^{*(m)} \right\|_{\ell_1/\mathbb{K}}.$$

Combining these, we get

$$\left\| \tilde{\boldsymbol{\beta}}^{(m)} \right\|_{\ell_1/\mathbb{K}} \geq \left\| \boldsymbol{\beta}_{\mathcal{A}^{(m)}}^{*(m)} \right\|_{\ell_1/\mathbb{K}} - \left\| \tilde{\boldsymbol{\beta}}_{\mathcal{A}^{(m)}}^{(m)} - \boldsymbol{\beta}_{\mathcal{A}^{(m)}}^{*(m)} \right\|_{\ell_1/\mathbb{K}} + \left\| \tilde{\boldsymbol{\beta}}_{\mathcal{A}^{(m)C}}^{(m)} \right\|_{\ell_1/\mathbb{K}}.$$

Also, note that

$$\left\| \tilde{\boldsymbol{\beta}}^{(m)} - \boldsymbol{\beta}^{*(m)} \right\|_{\ell_1/\mathbb{K}} = \left\| \tilde{\boldsymbol{\beta}}_{\mathcal{A}^{(m)}}^{(m)} - \boldsymbol{\beta}_{\mathcal{A}^{(m)}}^{*(m)} \right\|_{\ell_1/\mathbb{K}} + \left\| \tilde{\boldsymbol{\beta}}_{\mathcal{A}^{(m)C}}^{(m)} \right\|_{\ell_1/\mathbb{K}}.$$

By substitution into the inequality (S1), we conclude that

$$\begin{aligned} \left\| \hat{\Gamma}_{\mathbf{X}\mathbf{X}}^{(m)1/2} \left(\tilde{\boldsymbol{\beta}}^{(m)} - \boldsymbol{\beta}^{*(m)} \right) \right\|_{\mathbb{K}}^2 &\leq \lambda \left\| \tilde{\boldsymbol{\beta}}^{(m)} - \boldsymbol{\beta}^{*(m)} \right\|_{\ell_1/\mathbb{K}} + 2\lambda \left\| \boldsymbol{\beta}^{*(m)} \right\|_{\ell_1/\mathbb{K}} - 2\lambda \left\| \tilde{\boldsymbol{\beta}}^{(m)} \right\|_{\ell_1/\mathbb{K}} \\ &\leq \lambda \left(\left\| \tilde{\boldsymbol{\beta}}_{\mathcal{A}^{(m)}}^{(m)} - \boldsymbol{\beta}_{\mathcal{A}^{(m)}}^{*(m)} \right\|_{\ell_1/\mathbb{K}} + \left\| \tilde{\boldsymbol{\beta}}_{\mathcal{A}^{(m)C}}^{(m)} \right\|_{\ell_1/\mathbb{K}} \right) + 2\lambda \left\| \boldsymbol{\beta}_{\mathcal{A}^{(m)C}}^{*(m)} \right\|_{\ell_1/\mathbb{K}} \\ &\quad - 2\lambda \left(\left\| \boldsymbol{\beta}_{\mathcal{A}^{(m)}}^{*(m)} \right\|_{\ell_1/\mathbb{K}} - \left\| \tilde{\boldsymbol{\beta}}_{\mathcal{A}^{(m)}}^{(m)} - \boldsymbol{\beta}_{\mathcal{A}^{(m)}}^{*(m)} \right\|_{\ell_1/\mathbb{K}} + \left\| \tilde{\boldsymbol{\beta}}_{\mathcal{A}^{(m)C}}^{(m)} \right\|_{\ell_1/\mathbb{K}} \right). \end{aligned}$$

Simplification and rearrangement yield the desired result. \square

Proof of Theorem 1.

Proof. We start with the decomposition

$$\begin{aligned} & \left\| \hat{\Gamma}_{\mathbf{X}\mathbf{X}}^{(m)1/2} \left(\tilde{\beta}^{(m)} - \beta^{*(m)} \right) \right\|_{\mathbb{K}}^2 + \lambda \left\| \tilde{\beta}^{(m)} - \beta^{*(m)} \right\|_{\ell_1/\mathbb{K}} = \left\| \hat{\Gamma}_{\mathbf{X}\mathbf{X}}^{(m)1/2} \left(\tilde{\beta}^{(m)} - \beta^{*(m)} \right) \right\|_{\mathbb{K}}^2 \\ & \quad + \lambda \left\| \left(\tilde{\beta}^{(m)} - \beta^{*(m)} \right)_{\mathcal{A}^{(m)}} \right\|_{\ell_1/\mathbb{K}} + \lambda \left\| \tilde{\beta}_{\mathcal{A}^{(m)C}}^{(m)} \right\|_{\ell_1/\mathbb{K}}. \end{aligned}$$

By using Lemmas S1 and S2, with probability at least $1 - \delta$, we have

$$\begin{aligned} & \left\| \hat{\Gamma}_{\mathbf{X}\mathbf{X}}^{(m)1/2} \left(\tilde{\beta}^{(m)} - \beta^{*(m)} \right) \right\|_{\mathbb{K}}^2 + \lambda \left\| \left(\tilde{\beta}^{(m)} - \beta^{*(m)} \right)_{\mathcal{A}^{(m)}} \right\|_{\ell_1/\mathbb{K}} + \lambda \left\| \tilde{\beta}_{\mathcal{A}^{(m)C}}^{(m)} \right\|_{\ell_1/\mathbb{K}} \quad (\text{S2}) \\ & \leq 4\lambda \left\| \left(\tilde{\beta}^{(m)} - \beta^{*(m)} \right)_{\mathcal{A}^{(m)}} \right\|_{\ell_1/\mathbb{K}}. \end{aligned}$$

Now, using the relation between the ℓ_1 and ℓ_2 norms, we can further bound the right-hand side:

$$4\lambda \left\| \left(\tilde{\beta}^{(m)} - \beta^{*(m)} \right)_{\mathcal{A}^{(m)}} \right\|_{\ell_1/\mathbb{K}} \leq 4\lambda\sqrt{p_0} \left\| \left(\tilde{\beta}^{(m)} - \beta^{*(m)} \right)_{\mathcal{A}^{(m)}} \right\|_{\mathbb{K}}.$$

Next, we use Assumption 3:

$$4\lambda\sqrt{p_0} \left\| \left(\tilde{\beta}^{(m)} - \beta^{*(m)} \right)_{\mathcal{A}^{(m)}} \right\|_{\mathbb{K}} \leq \frac{4\lambda\sqrt{p_0}}{\alpha_m} \left\| \hat{\Gamma}_{\mathbf{X}\mathbf{X}}^{(m)1/2} \left(\tilde{\beta}^{(m)} - \beta^{*(m)} \right) \right\|_{\mathbb{K}}.$$

Using the inequality $2ab \leq a^2 + b^2$ for real numbers, we further bound the right-hand side:

$$\frac{4\lambda\sqrt{p_0}}{\alpha_m} \left\| \hat{\Gamma}_{\mathbf{X}\mathbf{X}}^{(m)1/2} \left(\tilde{\beta}^{(m)} - \beta^{*(m)} \right) \right\|_{\mathbb{K}} \leq \frac{1}{2} \left\| \hat{\Gamma}_{\mathbf{X}\mathbf{X}}^{(m)1/2} \left(\tilde{\beta}^{(m)} - \beta^{*(m)} \right) \right\|_{\mathbb{K}}^2 + \frac{8\lambda^2 p_0}{\alpha_m^2}.$$

By substitution in the inequality (S2), we obtain

$$\begin{aligned} & \left\| \hat{\Gamma}_{\mathbf{X}\mathbf{X}}^{(m)1/2} \left(\tilde{\beta}^{(m)} - \beta^{*(m)} \right) \right\|_{\mathbb{K}}^2 + \lambda \left\| \left(\tilde{\beta}^{(m)} - \beta^{*(m)} \right)_{\mathcal{A}^{(m)}} \right\|_{\ell_1/\mathbb{K}} + \lambda \left\| \tilde{\beta}_{\mathcal{A}^{(m)C}}^{(m)} \right\|_{\ell_1/\mathbb{K}} \\ & \leq \frac{1}{2} \left\| \hat{\Gamma}_{\mathbf{X}\mathbf{X}}^{(m)1/2} \left(\tilde{\beta}^{(m)} - \beta^{*(m)} \right) \right\|_{\mathbb{K}}^2 + \frac{8\lambda^2 p_0}{\alpha_m^2}. \end{aligned}$$

Rearranging terms, we conclude that, with probability at least $1 - \delta$,

$$\frac{1}{2} \left\| \hat{\Gamma}_{\mathbf{X}\mathbf{X}}^{(m)1/2} \left(\tilde{\beta}^{(m)} - \beta^{*(m)} \right) \right\|_{\mathbb{K}}^2 + \lambda \left\| \tilde{\beta}^{(m)} - \beta^{*(m)} \right\|_{\ell_1/\mathbb{K}} \leq \frac{8\lambda^2 p_0}{\alpha_m^2}.$$

□

S1.6 Functional subgradient

To prove Theorem 2, we first need to compute the functional subgradient of the objective function (7). Lemma S3 establishes a simple but crucial connection between the inner products in \mathbb{H} and \mathbb{K} , which allows us to bridge the gap between these spaces.

Lemma S3. *Let $x \in \mathbb{K}$ and $z \in \mathbb{H}$. Then, the subgradient of $\langle x, z \rangle_{\mathbb{H}}$ with respect to x in \mathbb{K} is the singleton $\{K(z)\}$.*

Proof. By Proposition S1, for $z \in \mathbb{H}$, the relation $\|K^{1/2}(z)\|_{\mathbb{K}} = \|z\|_{\mathbb{H}}$ holds. Using the polarization identity, we express the inner product in terms of the norm:

$$\begin{aligned} \langle x, z \rangle_{\mathbb{H}} &= \frac{1}{4} \left(\|x + z\|_{\mathbb{H}}^2 - \|x - z\|_{\mathbb{H}}^2 \right) = \frac{1}{4} \left(\|K^{1/2}(x + z)\|_{\mathbb{K}}^2 - \|K^{1/2}(x - z)\|_{\mathbb{K}}^2 \right) \\ &= \left\langle K^{1/2}(x), K^{1/2}(z) \right\rangle_{\mathbb{K}} = \langle x, K(z) \rangle_{\mathbb{K}}. \end{aligned}$$

Now, let $f(x) = \langle x, z \rangle_{\mathbb{H}}$. For any $y \in \mathbb{K}$

$$f(x + y) - f(x) = \langle x + y, z \rangle_{\mathbb{H}} - \langle x, z \rangle_{\mathbb{H}} = \langle y, z \rangle_{\mathbb{H}} = \langle K(z), y \rangle_{\mathbb{K}}.$$

Thus, $K(z)$ is a subgradient of f at x . To show that $K(z)$ is the full subdifferential of f at x , consider $w \neq K(z)$ in \mathbb{K} . By Riesz representation theorem, there exists a $y \in \mathbb{K}$ such that $\langle y, K(z) - w \rangle_{\mathbb{K}} \neq 0$. Hence, no other vector $w \neq K(z)$ satisfies the subgradient inequality for all y . \square

We can now compute the subgradient of the function (7) using basic tools of convex analysis. For the square error part of the objective function, the subgradient can be computed using Lemma S3, combined with the additivity and linearity of subdifferentials in the following way:

$$\frac{\partial}{\partial \beta_j} \frac{1}{2n} \sum_{i=1}^n \left(Y_i - \sum_{k=1}^p \langle \beta_k, X_{ik}^{(m)} \rangle_{\mathbb{H}} \right)^2 = -\frac{1}{n} \left(\sum_{i=1}^n \left(Y_i - \sum_{k=1}^p \langle \beta_k, K(X_{ik}^{(m)}) \rangle_{\mathbb{K}} \right) K(X_{ij}^{(m)}) \right).$$

The subgradient of the second part can be computed using Section A.1 in Fan and Reimherr (2017):

$$\frac{\partial}{\partial \beta_j} \lambda \sum_{k=1}^p \tilde{w}_k \|\beta_k\|_{\mathbb{K}} = \lambda \tilde{w}_j \begin{cases} \|\beta_j\|_{\mathbb{K}}^{-1} \beta_j & \text{if } \beta_j \neq 0, \\ \{h \in \mathbb{H} : \|h\|_{\mathbb{K}} \leq 1\} & \text{if } \beta_j = 0. \end{cases}$$

Finally, the subgradient of the entire function is the sum of these two:

$$\begin{aligned} \frac{\partial}{\partial \beta_j} L_{\lambda}(\beta) &= -\frac{1}{n} \left(\sum_{i=1}^n \left(Y_i - \sum_{k=1}^p \langle \beta_k, K(X_{ik}^{(m)}) \rangle_{\mathbb{K}} \right) K(X_{ij}^{(m)}) \right) \\ &\quad + \lambda \tilde{w}_j \begin{cases} \|\beta_j\|_{\mathbb{K}}^{-1} \beta_j & \text{if } \beta_j \neq 0, \\ \{h \in \mathbb{K} : \|h\|_{\mathbb{K}} \leq 1\} & \text{if } \beta_j = 0. \end{cases} \end{aligned}$$

Note that β_j is an element of $\mathbb{K}^{(m)}$ and the function L_{λ} is defined over $\mathbb{K}^{(m)}$. Therefore, the subgradient is a set of elements of $\mathbb{K}^{(m)}$.

S1.7 Proof of Theorem 2

Proof.

(i) If $j \in \mathcal{A}^c$, then $\beta_j^* = 0$ and hence $\beta_j^{*(m)} = 0$ for all m . So, $\mathcal{A}^{(m)} \subseteq \mathcal{A}$. If $j \in \mathcal{A}$, then, by point 2 of Assumption 4, uniformly on $j \in \mathcal{A}$ we have

$$\|\beta_j^{*(m)}\|_{\mathbb{K}} \geq \|\beta_j^*\|_{\mathbb{K}} - \|\beta_j^* - \beta_j^{*(m)}\|_{\mathbb{K}} \geq b - o(b) = (1 - o(1))b.$$

Hence, there exists m_0 such that $\|\beta_j^{*(m)}\|_{\mathbb{K}} \geq b/2 > 0$ for all $m \geq m_0$ and all $j \in \mathcal{A}$, which implies $\mathcal{A} \subseteq \mathcal{A}^{(m)}$ for all $m \geq m_0$. Combining both inclusions yields $\mathcal{A}^{(m)} = \mathcal{A}$ for all large m . Thus, it is sufficient to prove that, as the sample size grows, $\mathbb{P}(\hat{\mathcal{A}}^{(m)} = \mathcal{A}^{(m)}) \rightarrow 1$.

We show that, as the sample size grows, with probability tending to 1, the following holds:

$$\hat{\beta}_j^{(m)} \neq 0 \quad \text{for } j \in \mathcal{A}^{(m)} \quad \text{and} \quad \hat{\beta}_j^{(m)} = 0 \quad \text{for } j \in \mathcal{A}^{(m)c},$$

where $\mathcal{A}^{(m)c}$ is the complement of $\mathcal{A}^{(m)}$ in $\{1, \dots, p\}$.

Consider the event $\{\hat{\mathcal{A}}^{(m)} = \mathcal{A}^{(m)}\}$. From Appendix S1.6 we see that, for all $j = 1, \dots, p$,

$$\sum_{i=1}^n \left(\left(Y_i - \sum_{k \in \mathcal{A}^{(m)}} \langle \hat{\beta}_k^{(m)}, K(X_{ik}^{(m)}) \rangle_{\mathbb{K}} \right) K(X_{ij}^{(m)}) \right) = \lambda \tilde{s}_j,$$

where

$$\tilde{s}_j = n \tilde{w}_j \begin{cases} \|\hat{\beta}_j^{(m)}\|_{\mathbb{K}}^{-1} \hat{\beta}_j^{(m)} & \text{if } \hat{\beta}_j^{(m)} \neq 0, \\ \{h \in \mathbb{K}^{(m)} : \|h\|_{\mathbb{K}} \leq 1\} & \text{if } \hat{\beta}_j^{(m)} = 0. \end{cases}$$

Using eq. (6), we can write

$$Y_i - \sum_{k \in \mathcal{A}^{(m)}} \langle \hat{\beta}_k^{(m)}, K(X_{ik}^{(m)}) \rangle_{\mathbb{K}} = \varepsilon_i - \sum_{k \in \mathcal{A}^{(m)}} \langle \hat{\beta}_k^{(m)} - \beta_k^{*(m)}, K(X_{ik}^{(m)}) \rangle_{\mathbb{K}}.$$

By substitution, we get

$$\sum_{i=1}^n \left(\varepsilon_i - \sum_{k \in \mathcal{A}^{(m)}} \langle \hat{\beta}_k^{(m)} - \beta_k^{*(m)}, K(X_{ik}^{(m)}) \rangle_{\mathbb{K}} \right) K(X_{ij}^{(m)}) = \lambda \tilde{s}_j.$$

For $j = 1, \dots, p$, we define $S_j : \mathbb{K}^{(m)} \rightarrow \mathbb{R}^n$ by $(S_j(\beta))_i = \langle \beta, K(X_{ij}^{(m)}) \rangle_{\mathbb{K}}$ and $S_j^* : \mathbb{R}^n \rightarrow \mathbb{K}^{(m)}$ by $S_j^*(y) = n^{-1} \sum_{i=1}^n y_i K(X_{ij}^{(m)})$. Moreover, on the set of active predictors, we define $\mathbf{S}_1 : \mathbb{K}^{(m)p_0} \rightarrow \mathbb{R}^n$ and $\mathbf{S}_1^* : \mathbb{R}^n \rightarrow \mathbb{K}^{(m)p_0}$ component-wise. Then, for $j, k = 1, \dots, p$, $S_j^* S_k = \hat{\Gamma}_{jk}^{(m)}$ and $\mathbf{S}_1^* \mathbf{S}_1 = \hat{\Gamma}_{\mathbf{X}_1}^{(m)}$. By using this notation and the tensor product definition of the covariance operator, the last equation can be written as

$$n S_j^*(\varepsilon) - n \sum_{k \in \mathcal{A}^{(m)}} \hat{\Gamma}_{jk}^{(m)} (\hat{\beta}_k^{(m)} - \beta_k^{*(m)}) = \lambda \tilde{s}_j, \quad j = 1, \dots, p. \quad (\text{S3})$$

This equation restricted to $j \in \mathcal{A}^{(m)}$ becomes

$$n \mathbf{S}_1^*(\varepsilon) - n \hat{\Gamma}_{\mathbf{X}_1}^{(m)} (\hat{\beta}_1^{(m)} - \beta_1^{*(m)}) = \lambda \tilde{\mathbf{s}}_1,$$

where $\hat{\beta}_1^{(m)} = \{\hat{\beta}_j^{(m)} : j \in \mathcal{A}^{(m)}\}$ and $\tilde{\mathbf{s}}_1 = \{n \tilde{w}_j \hat{\beta}_j^{(m)} \|\hat{\beta}_j^{(m)}\|_{\mathbb{K}}^{-1} : j \in \mathcal{A}^{(m)}\}$. So, the difference between the estimated and the true active coefficients can be formulated as

$$\hat{\beta}_1^{(m)} - \beta_1^{*(m)} = \hat{\Gamma}_{\mathbf{X}_1}^{(m)-1} \mathbf{S}_1^*(\varepsilon) - \lambda n^{-1} \hat{\Gamma}_{\mathbf{X}_1}^{(m)-1} \tilde{\mathbf{s}}_1. \quad (\text{S4})$$

However, trivially, $\hat{\beta}_j^{(m)} \neq 0$ if $\|\beta_j^{*(m)} - \hat{\beta}_j^{(m)}\|_{\mathbb{K}} < \|\beta_j^{*(m)}\|_{\mathbb{K}}$. By substituting eq. (S4) in the latter, we have to show that

$$\left\| e_j^\top \hat{\Gamma}_{\mathbf{X}_1}^{(m)-1} \mathbf{S}_1^*(\varepsilon) - \lambda n^{-1} e_j^\top \hat{\Gamma}_{\mathbf{X}_1}^{(m)-1}(\tilde{\mathbf{s}}_1) \right\|_{\mathbb{K}} < \left\| \beta_j^{*(m)} \right\|_{\mathbb{K}}, \quad (\text{S5})$$

where e_j is a vector with 1 in the j^{th} coordinate and zero everywhere else.

Now, we move to the null part. For $j \in \mathcal{A}^{(m)c}$, we have to show that $\hat{\beta}_j^{(m)}$ is equal to zero. From eq. (S3), it is sufficient to prove that

$$\left\| n S_j^*(\varepsilon) - n \sum_{k \in \mathcal{A}^{(m)}} \hat{\Gamma}_{jk}^{(m)} \left(\hat{\beta}_k^{(m)} - \beta_k^{*(m)} \right) \right\|_{\mathbb{K}} < n \lambda \tilde{w}_j.$$

By some simplification, we can write

$$\left\| S_j^*(\varepsilon) - e_j^\top \hat{\Gamma}_{\mathbf{X}_2 \mathbf{X}_1}^{(m)} \left(\hat{\beta}_1^{(m)} - \beta_1^{*(m)} \right) \right\|_{\mathbb{K}} < \lambda \tilde{w}_j.$$

This can be written in the form

$$\left\| S_j^*(\varepsilon) - n^{-1} e_j^\top \hat{\Gamma}_{\mathbf{X}_2 \mathbf{X}_1}^{(m)} \hat{\Gamma}_{\mathbf{X}_1}^{(m)-1} (\mathbf{S}_1^* \varepsilon - \tilde{\mathbf{s}}_1) \right\|_{\mathbb{K}} < \lambda \tilde{w}_j$$

or, equivalently,

$$\left\| S_j^* \left(\varepsilon - n^{-1} \mathbf{S}_1 \hat{\Gamma}_{\mathbf{X}_1}^{(m)-1} (\mathbf{S}_1^* \varepsilon - \lambda \tilde{\mathbf{s}}_1) \right) \right\|_{\mathbb{K}} < \lambda \tilde{w}_j.$$

Let I be the identity operator on \mathbb{R}^n and $H := I - \mathbf{S}_1 \hat{\Gamma}_{\mathbf{X}_1}^{(m)-1} \mathbf{S}_1^*$ the projector on the null space of \mathbf{S}_1 . Then,

$$\left\| S_j^* H(\varepsilon) + \lambda n^{-1} S_j^* \mathbf{S}_1 \hat{\Gamma}_{\mathbf{X}_1}^{(m)-1}(\tilde{\mathbf{s}}_1) \right\|_{\mathbb{K}} < \lambda \tilde{w}_j, \quad j \in \mathcal{A}^{(m)c}. \quad (\text{S6})$$

The inequality (S5) and (S6) indicate that $\hat{\mathcal{A}}^{(m)} = \mathcal{A}^{(m)}$ if the following two inequalities are satisfied:

$$\begin{cases} \left\| e_j^\top \hat{\Gamma}_{\mathbf{X}_1}^{(m)-1} \mathbf{S}_1^*(\varepsilon) - \lambda n^{-1} e_j^\top \hat{\Gamma}_{\mathbf{X}_1}^{(m)-1}(\tilde{\mathbf{s}}_1) \right\|_{\mathbb{K}} < \left\| \beta_j^{*(m)} \right\|_{\mathbb{K}}, & j \in \mathcal{A}^{(m)}, \\ \left\| S_j^* H(\varepsilon) + \lambda n^{-1} S_j^* \mathbf{S}_1 \hat{\Gamma}_{\mathbf{X}_1}^{(m)-1}(\tilde{\mathbf{s}}_1) \right\|_{\mathbb{K}} < \lambda \tilde{w}_j, & j \in \mathcal{A}^{(m)c}. \end{cases}$$

Therefore, the event $\{\hat{\mathcal{A}}^{(m)} \neq \mathcal{A}^{(m)}\}$ satisfies $\{\hat{\mathcal{A}}^{(m)} \neq \mathcal{A}^{(m)}\} \subset B_1 \cup B_2 \cup B_3 \cup B_4$, where B_1 to B_4 are the following subsets of indices:

$$\begin{aligned} B_1 &= \left\{ j \in \mathcal{A}^{(m)} : \left\| e_j^\top \hat{\Gamma}_{\mathbf{X}_1}^{(m)-1} \mathbf{S}_1^*(\varepsilon) \right\|_{\mathbb{K}} \geq \frac{\left\| \beta_j^{*(m)} \right\|_{\mathbb{K}}}{2} \right\}, \\ B_2 &= \left\{ j \in \mathcal{A}^{(m)} : \lambda n^{-1} \left\| e_j^\top \hat{\Gamma}_{\mathbf{X}_1}^{(m)-1}(\tilde{\mathbf{s}}_1) \right\|_{\mathbb{K}} \geq \frac{\left\| \beta_j^{*(m)} \right\|_{\mathbb{K}}}{2} \right\}, \\ B_3 &= \left\{ j \in \mathcal{A}^{(m)c} : \left\| S_j^* H(\varepsilon) \right\|_{\mathbb{K}} \geq \frac{\lambda \tilde{w}_j}{2} \right\}, \\ B_4 &= \left\{ j \in \mathcal{A}^{(m)c} : n^{-1} \left\| S_j^* \mathbf{S}_1 \hat{\Gamma}_{\mathbf{X}_1}^{(m)-1}(\tilde{\mathbf{s}}_1) \right\|_{\mathbb{K}} \geq \frac{\tilde{w}_j}{2} \right\}. \end{aligned}$$

We show that $\lim_{n \rightarrow +\infty} P(B_l) \rightarrow 0$ for $l = 1, \dots, 4$ in separate steps. This will complete the proof of (i).

Step 1: $P(B_1) \rightarrow 0$, as $n \rightarrow +\infty$.

First, observe that, from point 1 in Assumption 4, for all $j \in \mathcal{A}^{(m)}$,

$$\|e_j^\top \hat{\Gamma}_{\mathbf{X}_1}^{(m)-1} \mathbf{S}_1^*(\varepsilon)\|_{\mathbb{K}} \leq \|e_j^\top \hat{\Gamma}_{\mathbf{X}_1}^{(m)-1}\|_{\text{op}} \|\mathbf{S}_1^*(\varepsilon)\|_{\mathbb{K}} \leq \tau_m \sum_{k \in \mathcal{A}^{(m)}} \|\mathbf{S}_k^*(\varepsilon)\|_{\mathbb{K}}.$$

Moreover, using $\mathbf{S}_k^*(\varepsilon) = n^{-1} \sum_{i=1}^n \varepsilon_i K(X_{ik}^{(m)}) = n^{-1} K(Z_k)$ with $Z_k := \sum_{i=1}^n \varepsilon_i X_{ik}^{(m)}$, and the bound $\|K(h)\|_{\mathbb{K}} \leq \sqrt{\theta_1} \|h\|_{\mathbb{H}}$, we obtain

$$\|\mathbf{S}_k^*(\varepsilon)\|_{\mathbb{K}} = n^{-1} \|K(Z_k)\|_{\mathbb{K}} \leq \sqrt{\theta_1} n^{-1} \|Z_k\|_{\mathbb{H}}.$$

Hence, for any $j \in \mathcal{A}^{(m)}$,

$$\|e_j^\top \hat{\Gamma}_{\mathbf{X}_1}^{(m)-1} \mathbf{S}_1^*(\varepsilon)\|_{\mathbb{K}} \leq \sqrt{\theta_1} \tau_m n^{-1} \sum_{k \in \mathcal{A}^{(m)}} \|Z_k\|_{\mathbb{H}}.$$

By point 2 of Assumption 4 (minimum signal condition),

$$P(B_1) \leq \sum_{k \in \mathcal{A}^{(m)}} P\left(n^{-1} \sqrt{\theta_1} \tau_m \|Z_k\|_{\mathbb{H}} \geq \frac{b_m}{2}\right).$$

Using Assumption 1 and Lemma 1, we obtain for some constant $M > 0$,

$$\begin{aligned} P(B_1) &\leq \sum_{k \in \mathcal{A}^{(m)}} P\left(n^{-1} \left\| \sum_{i=1}^n \varepsilon_i X_{ik}^{(m)} \right\|_{\mathbb{H}} \geq \frac{b_m}{2\sqrt{\theta_1}\tau_m}\right) \leq \sum_{k \in \mathcal{A}^{(m)}} \exp\left(-\frac{b_m^2 n}{4\theta_1 \tau_m^2 M}\right) \\ &= p_0 \exp\left(-\frac{b_m^2 n}{4\theta_1 \tau_m^2 M}\right) = \exp\left(-\frac{b_m^2 n}{4\theta_1 \tau_m^2 M} + \log(p_0)\right). \end{aligned}$$

The last term tends to zero, as $n \rightarrow +\infty$, because, by the minimum signal assumption, $\log(p_0) \ll \frac{b_m^2 n}{\tau_m^2}$.

Step 2: $P(B_2) \rightarrow 0$, when $n \rightarrow +\infty$.

We begin by evaluating the \mathbb{K} -norm of $\tilde{\mathbf{s}}_1$:

$$\|\tilde{\mathbf{s}}_1\|_{\mathbb{K}}^2 = n^2 \sum_{j \in \mathcal{A}^{(m)}} \tilde{w}_j^2 = n^2 \sum_{j \in \mathcal{A}^{(m)}} w_j^2 + n^2 \sum_{j \in \mathcal{A}^{(m)}} (\tilde{w}_j^2 - w_j^2),$$

where $\tilde{w}_j = \|\tilde{\beta}_j^{(m)}\|_{\mathbb{K}}^{-1}$ and $w_j = \|\beta_j^{*(m)}\|_{\mathbb{K}}^{-1}$. For the difference $\tilde{w}_j^2 - w_j^2$, we write

$$\tilde{w}_j^2 - w_j^2 = \|\tilde{\beta}_j^{(m)}\|_{\mathbb{K}}^{-2} - \|\beta_j^{*(m)}\|_{\mathbb{K}}^{-2} = \frac{\|\beta_j^{*(m)}\|_{\mathbb{K}}^2 - \|\tilde{\beta}_j^{(m)}\|_{\mathbb{K}}^2}{\|\beta_j^{*(m)}\|_{\mathbb{K}}^2 \|\tilde{\beta}_j^{(m)}\|_{\mathbb{K}}^2}.$$

By factoring in the numerator, we have

$$\tilde{w}_j^2 - w_j^2 = \frac{\left(\|\beta_j^{*(m)}\|_{\mathbb{K}} - \|\tilde{\beta}_j^{(m)}\|_{\mathbb{K}}\right) \left(\|\beta_j^{*(m)}\|_{\mathbb{K}} + \|\tilde{\beta}_j^{(m)}\|_{\mathbb{K}}\right)}{\|\beta_j^{*(m)}\|_{\mathbb{K}}^2 \|\tilde{\beta}_j^{(m)}\|_{\mathbb{K}}^2}. \quad (\text{S7})$$

From Assumption 4 and Corollary 1, we know that $r_m^{1/2}/b_m \rightarrow 0$ when $n \rightarrow +\infty$. So,

$$\left\| \tilde{\beta}_j^{(m)} \right\|_{\mathbb{K}} \leq \left\| \beta_j^{*(m)} \right\|_{\mathbb{K}} + \left\| \tilde{\beta}_j^{(m)} - \beta_j^{*(m)} \right\|_{\mathbb{K}} = \left\| \beta_j^{*(m)} \right\|_{\mathbb{K}} (1 + o_P(1))$$

uniformly in j . By the reverse triangle inequality, we similarly find

$$\left\| \tilde{\beta}_j^{(m)} \right\|_{\mathbb{K}} \geq \left\| \beta_j^{*(m)} \right\|_{\mathbb{K}} - \left\| \tilde{\beta}_j^{(m)} - \beta_j^{*(m)} \right\|_{\mathbb{K}} = \left\| \beta_j^{*(m)} \right\|_{\mathbb{K}} (1 + o_P(1)).$$

Therefore,

$$\left| \left\| \beta_j^{*(m)} \right\|_{\mathbb{K}} - \left\| \tilde{\beta}_j^{(m)} \right\|_{\mathbb{K}} \right| \leq \left\| \tilde{\beta}_j^{(m)} - \beta_j^{*(m)} \right\|_{\mathbb{K}}.$$

By substituting these relations into eq. (S7), we obtain

$$|\tilde{w}_j^2 - w_j^2| = \frac{\left\| \beta_j^{*(m)} - \tilde{\beta}_j^{(m)} \right\|_{\mathbb{K}}}{\left\| \beta_j^{*(m)} \right\|_{\mathbb{K}}^3} (2 + o_P(1))$$

uniformly in j . Using the bound $b_m \leq \left\| \beta_j^{*(m)} \right\|_{\mathbb{K}}$ for all $j \in \mathcal{A}^{(m)}$, we find

$$|\tilde{w}_j^2 - w_j^2| \leq \frac{O_P(1)}{\left\| \beta_j^{*(m)} \right\|_{\mathbb{K}}^2 b_m} \left\| \beta_j^{*(m)} - \tilde{\beta}_j^{(m)} \right\|_{\mathbb{K}} \leq \frac{O_P(r_m^{1/2})}{b_m} w_j^2.$$

Since $r_m^{1/2}/b_m \rightarrow 0$ when $n \rightarrow +\infty$, we conclude that

$$\begin{aligned} \|\tilde{\mathbf{s}}_1\|_{\mathbb{K}}^2 &\leq n^2 \left(\sum_{j \in \mathcal{A}^{(m)}} w_j^2 \right) (1 + o_P(1)) = n^2 \left(\sum_{j \in \mathcal{A}^{(m)}} \frac{1}{\left\| \beta_j^{*(m)} \right\|_{\mathbb{K}}^2} \right) (1 + o_P(1)) \\ &\leq \frac{n^2 p_0}{b_m^2} (1 + o_P(1)). \end{aligned}$$

Now we return to the definition of B_2 . For each $j \in \mathcal{A}^{(m)}$,

$$\left\| e_j^\top \hat{\Gamma}_{\mathbf{X}_1}^{(m)-1} \tilde{\mathbf{s}}_1 \right\|_{\mathbb{K}} \leq \tau_m \|\tilde{\mathbf{s}}_1\|_{\mathbb{K}} \leq \frac{\tau_m n p_0^{1/2}}{b_m} (1 + o_P(1)).$$

Hence,

$$\begin{aligned} P(B_2) &\leq \sum_{j \in \mathcal{A}^{(m)}} P \left(n^{-1} \lambda \left\| e_j^\top \hat{\Gamma}_{\mathbf{X}_1}^{(m)-1} \tilde{\mathbf{s}}_1 \right\|_{\mathbb{K}} \geq \frac{\left\| \beta_j^{*(m)} \right\|_{\mathbb{K}}}{2} \right) \\ &\leq \sum_{j \in \mathcal{A}^{(m)}} P \left(\lambda \frac{\tau_m n p_0^{1/2}}{b_m n} (1 + o_P(1)) \geq \frac{b_m}{2} \right). \end{aligned}$$

By simplifying further, using point 4 in Assumption 4 and the fact that $p_0 \ll n$, we have

$$P(B_2) \leq p_0 P \left(\lambda \geq \frac{b_m^2}{2\tau_m p_0^{1/2}} \right) \rightarrow 0, \quad n \rightarrow +\infty,$$

where the limit is obtained by points 2 and 3 of Assumption 4:

$$\lambda \ll \frac{b_m}{p_0^{1/2} n^{1/2}} \ll \frac{b_m}{p_0^{1/2} n^{1/2}} \cdot \frac{b_m n^{1/2}}{\tau_m p_0 \log(p)^{1/2}} \leq \frac{b_m^2}{\tau_m p_0^{1/2}}.$$

Step 3: $P(B_3) \rightarrow 0$, as $n \rightarrow +\infty$.

For each $j \in \mathcal{A}^{(m)c}$, we consider $S_j^* H(\varepsilon) = n^{-1} \sum_{i=1}^n (H(\varepsilon))_i K(X_{ij}^{(m)})$. Using the bound $\|K(h)\|_{\mathbb{K}} \leq \sqrt{\theta_1} \|h\|_{\mathbb{H}}$,

$$\|S_j^* H(\varepsilon)\|_{\mathbb{K}} \leq \frac{\sqrt{\theta_1}}{n} \left\| \sum_{i=1}^n (H(\varepsilon))_i X_{ij}^{(m)} \right\|_{\mathbb{H}}.$$

We note that H is an orthogonal projector, hence $\|H\|_{\text{op}} \leq 1$. So, we can apply Lemma 1: for any $t > 0$,

$$\mathbb{P} \left(\frac{1}{n} \left\| \sum_{i=1}^n (H_n \varepsilon)_i X_{ij}^{(m)} \right\|_{\mathbb{H}} \geq t \right) \leq \exp \left(-\frac{n t^2}{M} \right).$$

Choosing $t = \lambda \tilde{w}_j / 2\sqrt{\theta_1}$ yields

$$\mathbb{P} \left(\|S_j^* H(\varepsilon)\|_{\mathbb{K}} \geq \frac{\lambda \tilde{w}_j}{2} \right) \leq \exp \left(-\frac{n \lambda^2 \tilde{w}_j^2}{4 \theta_1 M} \right).$$

By Corollary 1, for $j \in \mathcal{A}^{(m)c}$ there exists $C > 0$ such that $\sup_{j \in \mathcal{A}^{(m)c}} \|\tilde{\beta}_j^{(m)}\|_{\mathbb{K}} \leq C r_m^{1/2}$. Using the definition of \tilde{w}_j , we find $\tilde{w}_j = \|\tilde{\beta}_j^{(m)}\|_{\mathbb{K}}^{-1} \geq C^{-1} r_m^{-1/2}$. Hence,

$$\mathbb{P} \left(\|S_j^* H(\varepsilon)\|_{\mathbb{K}} \geq \frac{\lambda \tilde{w}_j}{2} \right) \leq \exp \left(-\frac{n \lambda^2}{4 \theta_1 M C^2 r_m} \right).$$

Taking a union bound over $j \in \mathcal{A}^{(m)c}$,

$$P(B_3) \leq (p - p_0) \exp \left(-\frac{n \lambda^2}{4 \theta_1 M C^2 r_m} \right) = \exp \left(-\frac{n \lambda^2}{4 \theta_1 M C^2 r_m} + \log((p - p_0)) \right).$$

To force $P(B_3) \rightarrow 0$, it suffices that, as $n \rightarrow +\infty$, $n \lambda^2 / r_m \gg \log(p)$. Since, by Corollary 1, $r_m = p_0 \log(p) / \alpha_m^2 n$, the right-hand side becomes

$$\frac{n \lambda^2}{r_m} = \frac{\lambda^2 \alpha_m^2 n^2}{p_0 \log(p)}.$$

Therefore, by the lower bound of λ in part 3 of Assumption 4

$$\frac{\lambda^2 \alpha_m^2 n^2}{p_0 \log(p)} \gg \frac{p_0 \log(p)^2 \alpha_m^2 n^2}{\zeta^2 n^2 p_0 \log(p)} \gg \log(p).$$

This ensures that $P(B_3) \rightarrow 0$ as $n \rightarrow +\infty$.

Step 4: $P(B_4) \rightarrow 0$, as $n \rightarrow +\infty$.

First, observe that, by point 4 of Assumption 4, uniformly on $j \in \mathcal{A}^{(m)c}$ we have

$$\|S_j^* \mathbf{S}_1 \hat{\Gamma}_{\mathbf{X}_1}^{(m)-1} \tilde{\mathbf{s}}_1\|_{\mathbb{K}} \leq \varphi_m \|\tilde{\mathbf{s}}_1\|_{\mathbb{K}} \leq \|\tilde{\mathbf{s}}_1\|_{\mathbb{K}}.$$

Thus, we can write

$$\begin{aligned} P(B_4) &\leq \sum_{j \in \mathcal{A}^{(m)c}} P\left(n^{-1} \left\| \mathbf{S}_j^* \mathbf{S}_1 \hat{\Gamma}_{\mathbf{X}_1}^{(m)-1}(\tilde{\mathbf{s}}_1) \right\|_{\mathbb{K}} \geq \frac{\tilde{w}_j}{2}\right) \\ &\leq \sum_{j \in \mathcal{A}^{(m)c}} P\left(n^{-1} \|\tilde{\mathbf{s}}_1\|_{\mathbb{K}} \geq \frac{\tilde{w}_j}{2\varphi_m}\right) \leq \sum_{j \in \mathcal{A}^{(m)c}} P\left(\frac{\|\tilde{\mathbf{s}}_1\|_{\mathbb{K}}}{n\tilde{w}_j} \geq \frac{1}{2}\right). \end{aligned}$$

Another use of Corollary 1 gives $\tilde{w}_j^{-1} = O_P(r_m^{1/2})$ for any $j \in \mathcal{A}^{(m)c}$. As a result, with probability tending to 1,

$$\frac{\|\tilde{\mathbf{s}}_1\|_{\mathbb{K}}}{n\tilde{w}_j} \ll \frac{p_0 \sqrt{\log(p)}}{b_m \alpha_m^2 \sqrt{n}}.$$

At this point, point 2 of Assumption 4 proves that $P(B_4) \rightarrow 0$ as $n \rightarrow +\infty$.

(ii) So far, we have shown that, with probability tending to 1, $\hat{\mathcal{A}}^{(m)} = \mathcal{A}^{(m)}$ and in this case the estimation takes the form $\hat{\boldsymbol{\beta}}^{(m)} = (\hat{\boldsymbol{\beta}}_1^{(m)}, 0)$. From eq. (S4) we know that

$$\hat{\boldsymbol{\beta}}_1^{(m)} = \boldsymbol{\beta}_1^{*(m)} + \hat{\Gamma}_{\mathbf{X}_1}^{(m)-1} \mathbf{S}_1^*(\varepsilon) - \lambda n^{-1} \hat{\Gamma}_{\mathbf{X}_1}^{(m)-1}(\tilde{\mathbf{s}}_1). \quad (\text{S8})$$

The oracle estimator is given by $\hat{\boldsymbol{\beta}}^{O(m)} = (\hat{\boldsymbol{\beta}}_1^{O(m)}, 0)$, where $\hat{\boldsymbol{\beta}}_1^{O(m)} = \Gamma_{\mathbf{X}_1}^{(m)-1} \Gamma_{Y\mathbf{X}_1}^{(m)}$. Using $Y = \sum_{k \in \mathcal{A}^{(m)}} \langle \beta_k^{*(m)}, K(X_{ik}^{(m)}) \rangle_{\mathbb{K}} + \varepsilon_i$, we have $\hat{\Gamma}_{Y\mathbf{X}_1}^{(m)} = \hat{\Gamma}_{\mathbf{X}_1}^{(m)} \boldsymbol{\beta}_1^{*(m)} + \mathbf{S}_1^*(\varepsilon)$. As a result,

$$\hat{\boldsymbol{\beta}}_1^{O(m)} = \boldsymbol{\beta}_1^{*(m)} + \hat{\Gamma}_{\mathbf{X}_1}^{(m)-1} \mathbf{S}_1^*(\varepsilon).$$

Combining eq. (S8) and the latter, we obtain

$$\hat{\boldsymbol{\beta}}_1^{O(m)} - \hat{\boldsymbol{\beta}}_1^{(m)} = \frac{\lambda}{n} \hat{\Gamma}_{\mathbf{X}_1}^{(m)-1}(\tilde{\mathbf{s}}_1).$$

Therefore,

$$\begin{aligned} \sqrt{n} \left\| \hat{\boldsymbol{\beta}}_1^{O(m)} - \hat{\boldsymbol{\beta}}_1^{(m)} \right\|_{\mathbb{K}} &= \sqrt{n} \left\| n^{-1} \lambda \hat{\Gamma}_{\mathbf{X}_1}^{(m)-1}(\tilde{\mathbf{s}}_1) \right\|_{\mathbb{K}} \leq \frac{\lambda \tau_m}{\sqrt{n}} \|\tilde{\mathbf{s}}_1\|_{\mathbb{K}} \\ &\leq \frac{\lambda \tau_m}{\sqrt{n}} \cdot \frac{n \sqrt{p_0}}{b_m} (1 + o_p(1)) \\ &= \frac{\lambda \tau_m \sqrt{p_0 n}}{b_m} (1 + o_p(1)) = o_p(\tau_m), \end{aligned}$$

where the last equality is true by point 3 of Assumption 4.

(iii) First, observe that

$$\sqrt{n} \left\| \hat{\boldsymbol{\beta}}_1^{(m)} - \hat{\boldsymbol{\beta}}_1^* \right\|_{\mathbb{K}} \leq \sqrt{n} \left\| \hat{\boldsymbol{\beta}}_1^{(m)} - \hat{\boldsymbol{\beta}}_1^{O(m)} \right\|_{\mathbb{K}} + \sqrt{n} \left\| \hat{\boldsymbol{\beta}}_1^{O(m)} - \boldsymbol{\beta}_1^* \right\|_{\mathbb{K}}.$$

In this equation, we already proved that $\sqrt{n} \left\| \hat{\boldsymbol{\beta}}_1^{(m)} - \hat{\boldsymbol{\beta}}_1^{O(m)} \right\|_{\mathbb{K}} = o_P(\tau_m)$. Regarding the second term, we first compute the expected value. For all $j \in \mathcal{A}^{(m)}$ and $l \in \mathbb{N}$,

$$\hat{\boldsymbol{\beta}}_1^{O(m)} = \boldsymbol{\beta}_1^{*(m)} + \hat{\Gamma}_{\mathbf{X}_1}^{(m)-1} \mathbf{S}_1^* \varepsilon,$$

$$\begin{aligned}
\mathbb{E} \left(\left\langle \hat{\beta}_j^{O(m)}, v_l \right\rangle_{\mathbb{K}} \right) &= \mathbb{E} \left(\left\langle \beta_j^{*(m)} + e_j \hat{\Gamma}_{\mathbf{X}_1}^{(m)-1} \mathbf{S}_1^*(\varepsilon), v_l \right\rangle_{\mathbb{K}} \right) \\
&= \mathbb{E} \left(\left\langle \beta_j^{*(m)}, v_l \right\rangle_{\mathbb{K}} \right) + \mathbb{E} \left(\left\langle e_j \hat{\Gamma}_{\mathbf{X}_1}^{(m)-1} \mathbf{S}_1^*(\varepsilon), v_l \right\rangle_{\mathbb{K}} \right) \\
&= \left\langle \beta_j^{*(m)}, v_l \right\rangle_{\mathbb{K}},
\end{aligned}$$

where the last equality holds because the design matrix is deterministic and ε is sub-Gaussian with mean zero. So,

$$\mathbb{E} \left(\left\langle \hat{\beta}_j^* - \hat{\beta}_j^{O(m)}, v_l \right\rangle_{\mathbb{K}} \right) = \left\langle \beta_j^{*(m)\perp}, v_l \right\rangle_{\mathbb{K}}.$$

By Markov's inequality, for any $\delta > 0$,

$$\begin{aligned}
P \left(n \left\| \hat{\beta}_j^* - \hat{\beta}_j^{O(m)} \right\|_{\mathbb{K}}^2 > \delta \right) &= P \left(\left\| \hat{\beta}_j^* - \hat{\beta}_j^{O(m)} \right\|_{\mathbb{K}}^2 > \frac{\delta}{n} \right) = P \left(\sum_{l=1}^{+\infty} \left\langle \hat{\beta}_j^* - \hat{\beta}_j^{O(m)}, v_l \right\rangle_{\mathbb{K}}^2 > \frac{\delta}{n} \right) \\
&\leq \frac{n^2}{\delta^2} \mathbb{E} \left(\sum_{l=1}^{+\infty} \left\langle \hat{\beta}_j^* - \hat{\beta}_j^{O(m)}, v_l \right\rangle_{\mathbb{K}}^2 \right) \leq \frac{n^2}{\delta^2} \left(\sum_{l=1}^{+\infty} \left\langle \hat{\beta}_j^{*(m)\perp}, v_l \right\rangle_{\mathbb{K}}^2 \right) \\
&\leq \frac{n^2}{\delta^2} \left\| \hat{\beta}_j^{*(m)\perp} \right\|_{\mathbb{K}}^2.
\end{aligned}$$

This means that $n \left\| \hat{\beta}_j^* - \hat{\beta}_j^{O(m)} \right\|_{\mathbb{K}}^2 = o_p(\tau_m^2 p_0^{-1})$ for all $j \in \mathcal{A}^{(m)}$. Finally,

$$\sqrt{n} \left\| \hat{\beta}_1^* - \hat{\beta}_1^{O(m)} \right\|_{\mathbb{K}} = \sum_{j \in \mathcal{A}^{(m)}} \left(n \left\| \hat{\beta}_j^* - \hat{\beta}_j^{O(m)} \right\|_{\mathbb{K}}^2 \right)^{\frac{1}{2}} \leq p_0 p_0^{-1} o_p(\tau_m) = o_p(\tau_m).$$

□

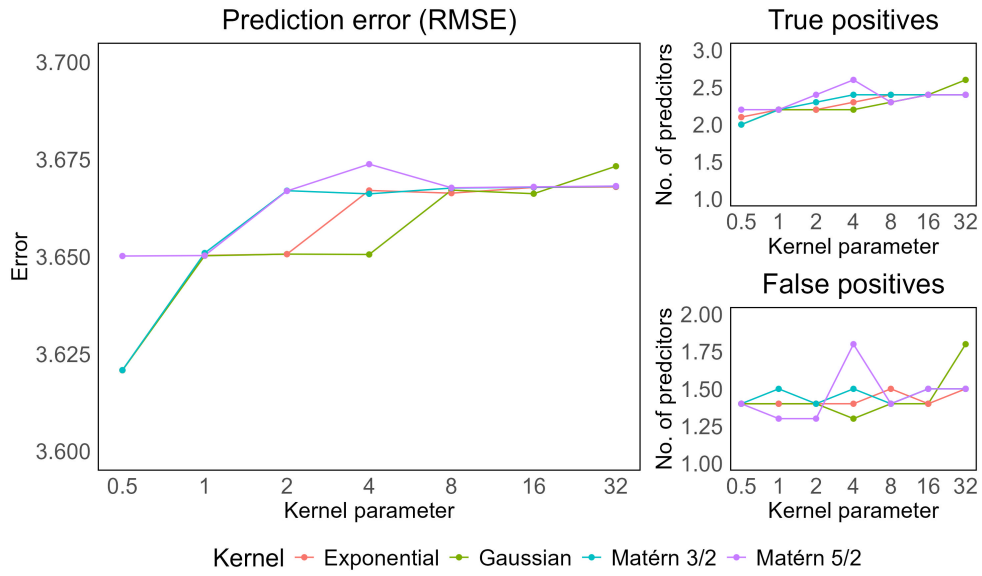
S2 Additional simulation results

S2.1 Performance and kernel comparison under extreme SNR levels

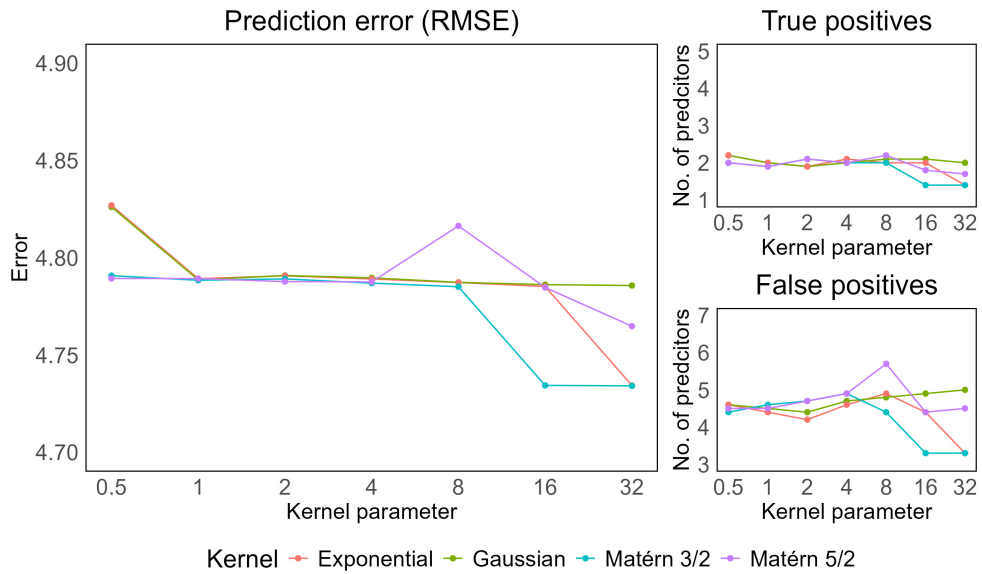
In this subsection, we present the performance of SOFIA under extreme SNR levels, i.e. SNR = 0.1, 0.5, and 100, for different kernel functions and kernel parameter values in the high-dimensional scale simulation scenarios (the results for SNR = 1 and 10 are shown in Figures 2 and 3, respectively).

Figures S1 and S2 illustrate the impact of very high noise (SNR = 0.1 and 0.5, respectively). As expected, as the SNR decreases, false positive rates increase, true positive rates decrease, and RMSE increases in both regimes. However, results remain pretty good also for SNR = 0.5, with a very small number of missed active predictors, and a small number of false positives. Figure S3 shows the near-noise-free setting (SNR = 100), where SOFIA achieves perfect performance with exact support recovery and minimal prediction error across all kernels and regimes. In all cases, although all kernel functions exhibit comparable performance, the Gaussian kernel tends to achieve slightly lower RMSE, indicating better prediction accuracy.

SNR = 0.1



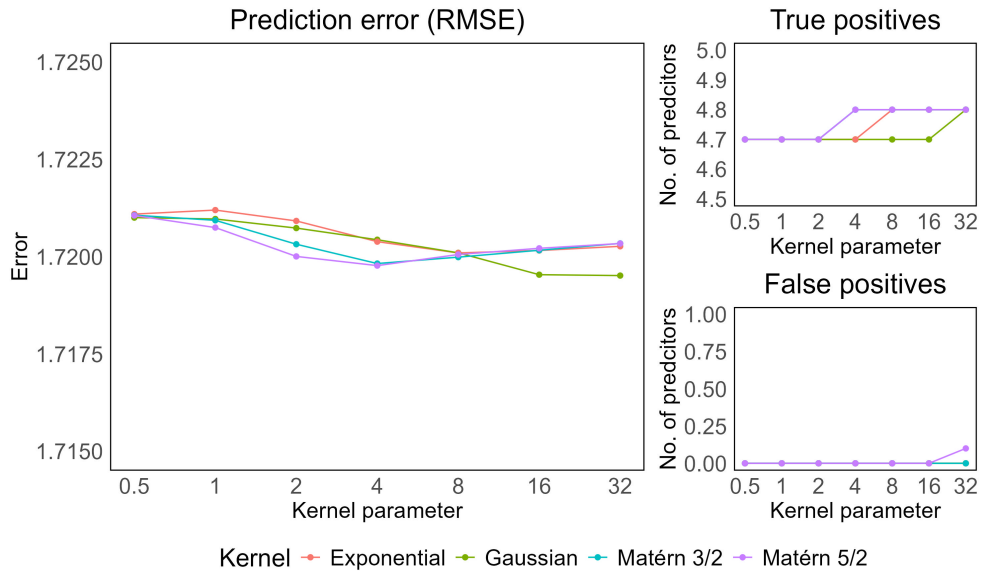
(a) Very sparse regime ($p_0 = 5$).



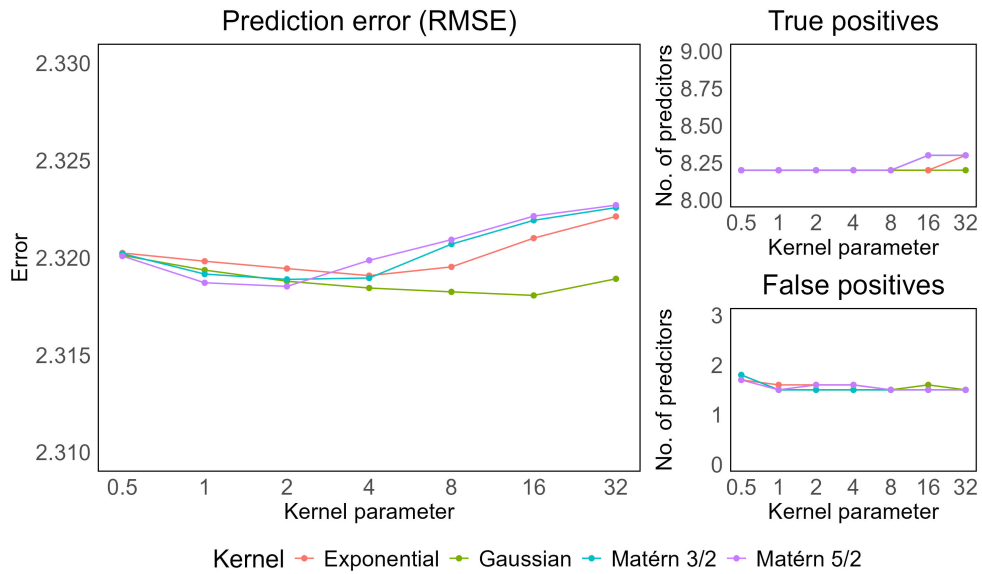
(b) Less sparse regime ($p_0 = 10$).

Figure S1: Comparison of the performance of different kernels under varying parameter values for SNR = 0.1. Subfigures represent the true positives, false positives, and root mean squared error (RMSE) in the very sparse and less sparse regimes, in the high-dimensional scale ($p = 700$).

SNR = 0.5



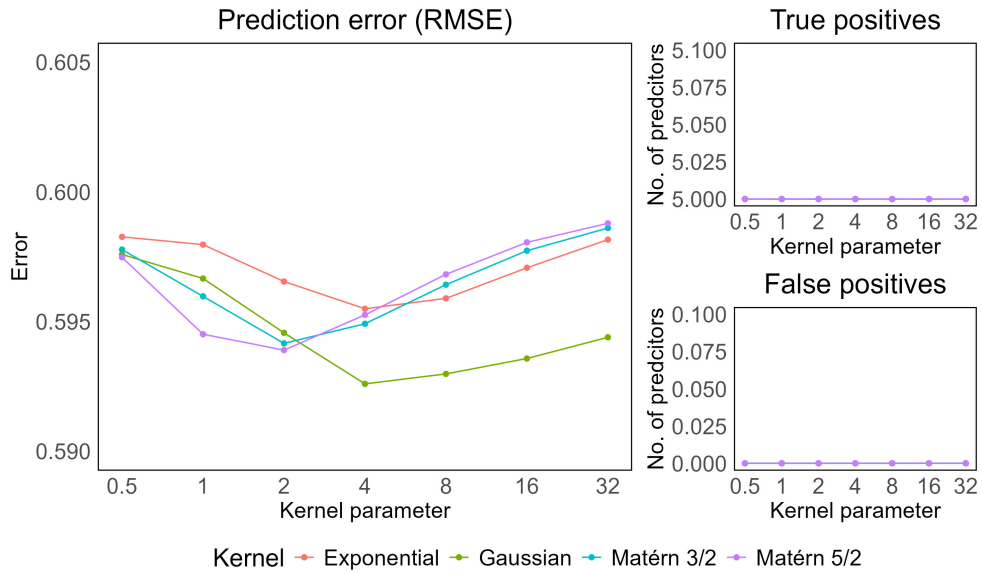
(a) Very sparse regime ($p_0 = 5$).



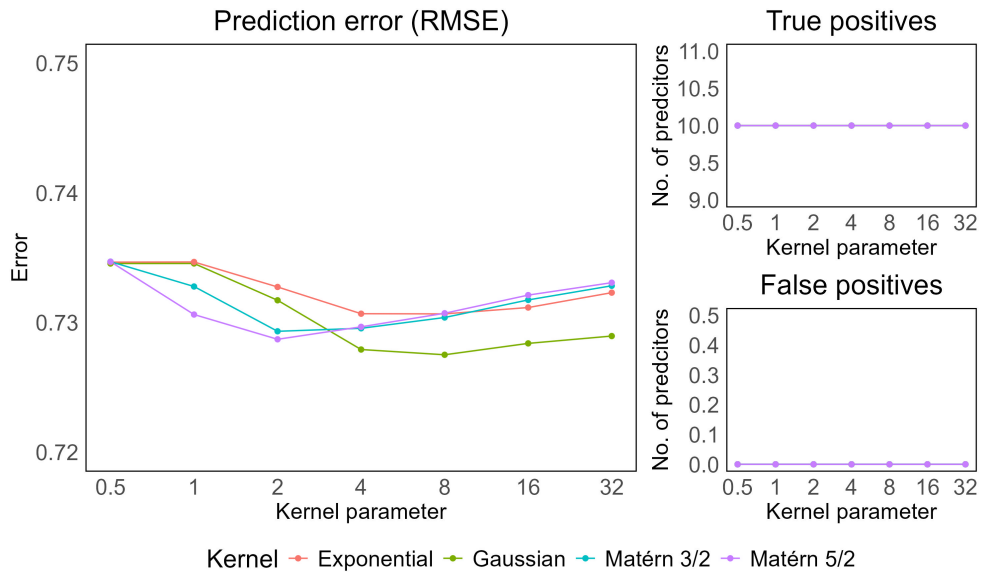
(b) Less sparse regime ($p_0 = 10$).

Figure S2: Comparison of the performance of different kernels under varying parameter values for SNR = 0.5. Subfigures represent the true positives, false positives, and root mean squared error (RMSE) in the very sparse and less sparse regimes, in the high-dimensional scale ($p = 700$).

SNR = 100



(a) Very sparse regime.



(b) Less sparse regime.

Figure S3: Comparison of the performance of different kernels under varying parameter values for SNR = 100. Subfigures represent the true positives, false positives, and root mean squared error (RMSE) in the very sparse and less sparse regimes, in the high-dimensional scale ($p = 700$).

S2.2 Estimated versus true coefficient functions

Figures S4 and S5 display the estimated coefficient functions $\hat{\beta}$ compared to the true β^* in the very sparse regime of the high-dimensional scale for $\text{SNR} = 1$ and $\text{SNR} = 10$, respectively. In particular, we report the results for the Gaussian kernel with $\rho = 8$ and the exponential kernel with $\rho = 2$. The Gaussian kernel produces smooth estimates with very limited fluctuation, while the exponential kernel exhibits noticeably more oscillations around the true coefficients. As expected, for a lower SNR level, the estimated coefficients are noisier; yet, SOFIA is still able to capture the main shapes and signs of the true coefficient functions.

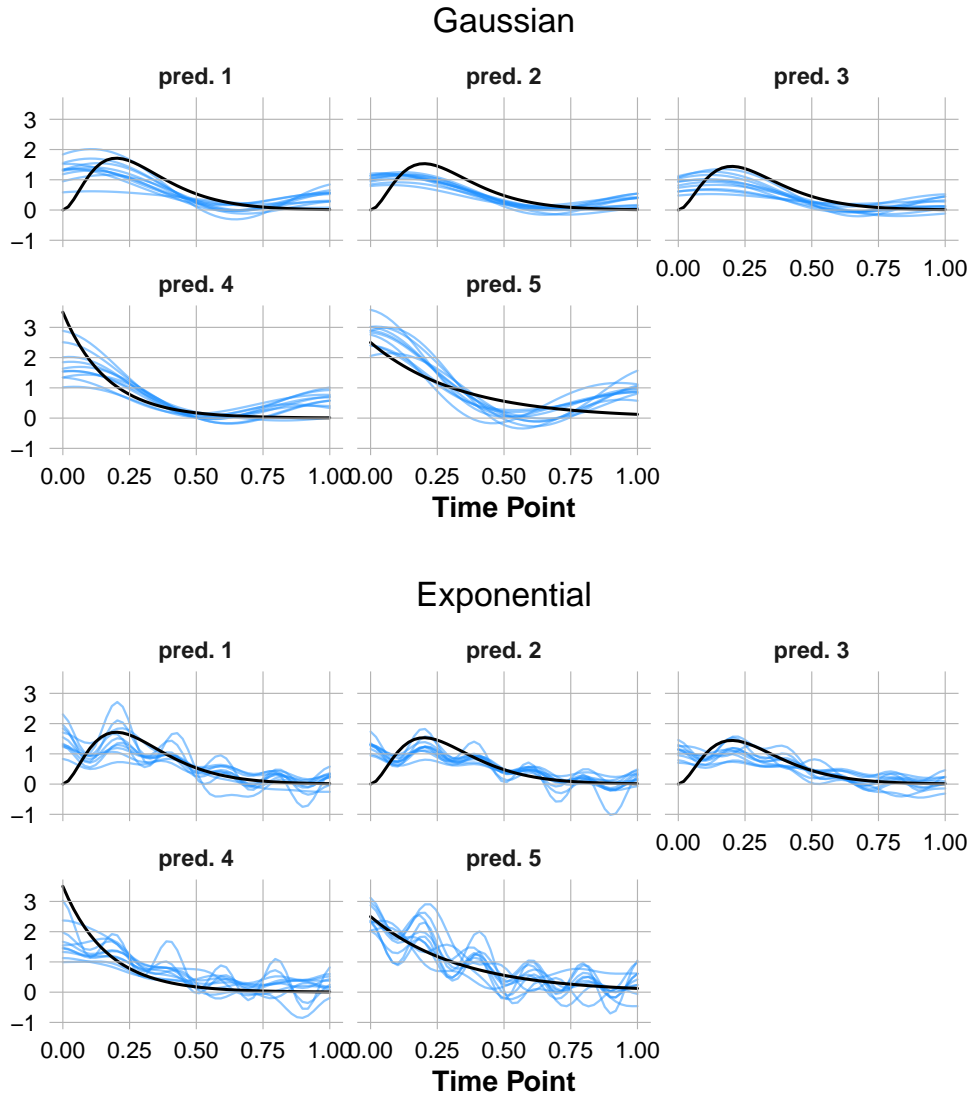


Figure S4: Estimated and true coefficient functions under $\text{SNR} = 1$ for the Gaussian kernel ($\rho = 8$) and the Exponential kernel ($\rho = 2$). True coefficients are shown in black, while blue curves represent the estimated coefficients across 10 runs.

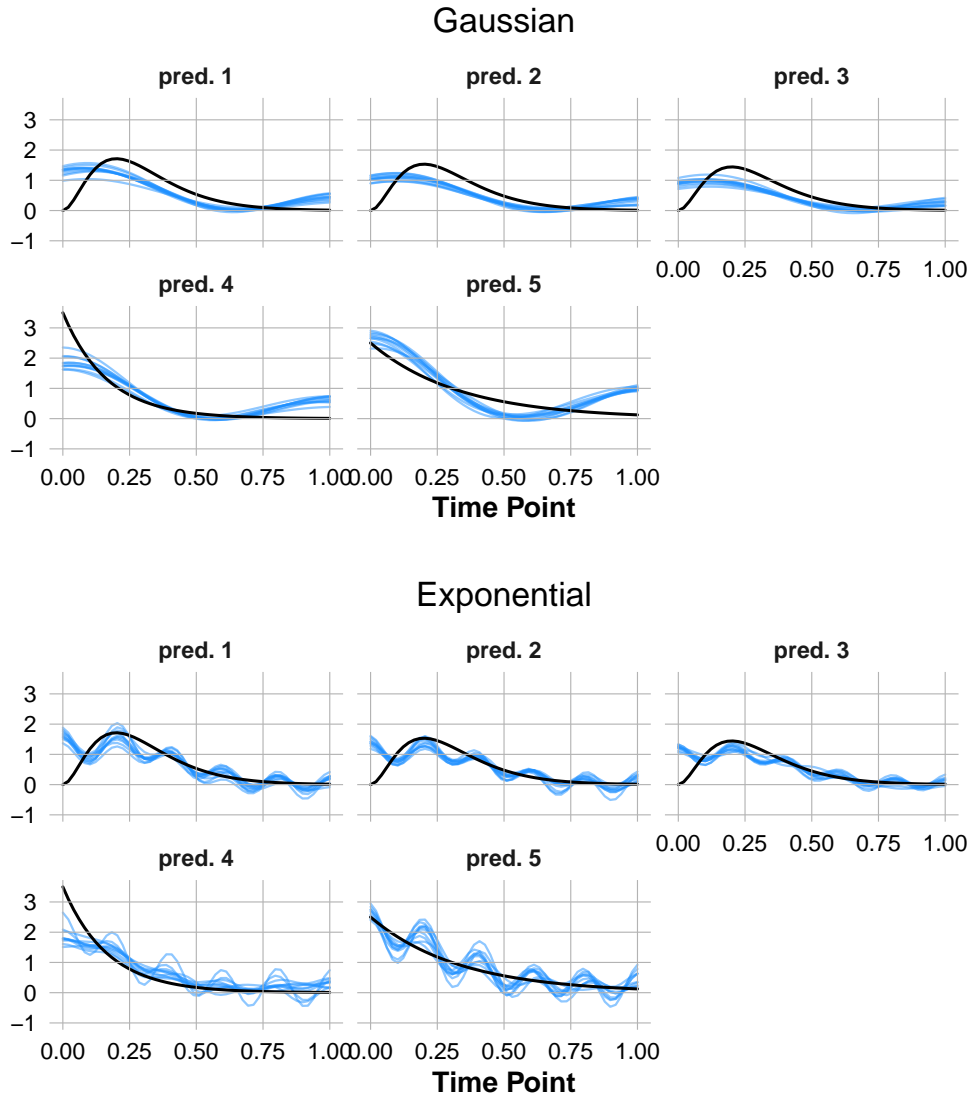


Figure S5: Estimated and true coefficient functions under $\text{SNR} = 10$ for the Gaussian kernel ($\rho = 8$) and the Exponential kernel ($\rho = 2$). True coefficients are shown in black, while blue curves represent the estimated coefficients across 10 runs.

References

- Barber, R. F., M. Reimherr, and T. Schill (2017). The function-on-scalar LASSO with applications to longitudinal GWAS. *Electronic Journal of Statistics* 11, 1351–1389.
- Fan, Z. and M. Reimherr (2017). High-dimensional adaptive function-on-scalar regression. *Econometrics and Statistics* 1, 167–183.
- Huang, J., S. Ma, and C.-H. Zhang (2008). Adaptive lasso for sparse high-dimensional regression models. *Statistica Sinica* 18, 1603–1618.
- Paulsen, V. I. and M. Raghupathi (2016). *An Introduction to the Theory of Reproducing Kernel Hilbert Spaces*, Volume 152. Cambridge University Press.
- Sarason, D. (2007). *Complex Function Theory* (2 ed.). American Mathematical Society.